Organometallics **2006,** *25,* 4118−4130

Chemistry of C-Trimethylsilyl-Substituted Heterocarboranes. 32. Synthetic and Structural Investigations on Half-Sandwich Lanthanacarboranes: Important Synthons in Metallacarborane Chemistry

Jianhui Wang,[†,‡] Joanna Smith,[†] Chong Zheng,[†] John A. Maguire,[‡] and
Narayan S. Hosmane*[,†]

Department of Chemistry and Biochemistry, Northern Illinois University, DeKalb, Illinois 60115-2862, and Department of Chemistry, Southern Methodist University, Dallas, Texas 75275-0314

Received March 24, 2006

The reactivities of the monosodium-complexed carborane precursors *nido*-1-Na(C_4H_8O)-2-(R)-3-($SiMe_3$)-2,3-$C_2B_4H_5$ (R = $SiMe_3$ (**1**) or Me (**2**)) with a number of lanthanide halides were investigated. The reaction of $LnCl_3$ (or $LnBr_3$) with **1** in a 1:2 molar ratio in dry THF at 60 °C produced the dimerized half-sandwich lanthanacarborane complexes [2,3-($SiMe_3$)$_2$-1-X-1-(THF)$_m$-1-Ln(η^5-2,3-$C_2B_4H_4$)]$_2$·*n*(THF) (**3**, Ln = Y, X = Cl, *m* = 2, *n* = 1; **4**, Ln = La, X = Br; *m* = 1, *n* = 0; **5**, Ln = Ce, X = Br; *m* = 1, *n* = 0; **6**, Ln = Pr, X = Br; *m* = 2, *n* = 1; **7**, Ln = Nd; X = Cl, *m* = 2, *n* = 1; **8**, Ln = Sm; X = Br, *m* = 2, *n* = 0; **9**, Ln = Gd; X = Cl, *m* = 2, *n* = 1; **10**, Ln = Tb, X = Cl, *m* = 2, *n* = 1; **11**, Ln = Dy, X = Cl, *m* = 2, *n* = 1; **12**, Ln = Ho, X = Cl, *m* = 2, *n* = 1; **13**, Ln = Er, X = Cl, *m* = 2, *n* = 1; **14**, Ln = Tm, X = Cl, *m* = 2, *n* = 1; **15**, Ln = Yb, X = Cl, *m* = 2, *n* = 1; **16**, Ln = Lu X = Cl, *m* = 2, *n* = 1) as crystalline solids in 70−92% isolated yields. In a similar manner, the reactions of **2** with $LnCl_3$ at 65 °C gave the corresponding complexes [2-Me-3-($SiMe_3$)-1-Cl-1-(THF)$_2$-1-Ln(η^5-2,3-$C_2B_4H_4$)]$_2$ (**17**, Ln = Nd; **18**, Ln = Dy; 1**9**, Ln = Ho; **20**, Ln = Er; **21**, Ln = Yb) as crystalline solids in 72−80% yield. In both series of the reactions, 1 equiv of the particular neutral carborane was also produced. The substitution of the chloride ions in complexes **17** and **20** by **2** gave the half-sandwich lanthanacarborane clusters {2-Me-3-($SiMe_3$)-1-[4,5-(μ-H)-*nido*-2-Me-3-($SiMe_3$)-2,3-$C_2B_4H_5$]-1-Ln(η^5-2,3-$C_2B_4H_4$)}$_2$·*n*(THF) (**22**, Ln = Nd, *n* = 2; **24**, Ln = Er, *n* = 1) as crystalline solids in 82−87% yield. The reaction of **19** and **2** produced the trimer {2-Me-3-($SiMe_3$)-1-[4,5-(μ-H)-*nido*-2-Me-3-($SiMe_3$)-2,3-$C_2B_4H_5$]-1-Ho(η^5-2,3-$C_2B_4H_4$)}$_3$·8(THF) (**23**) in 57% yield. Complexes **22**, **23**, and **24** could directly be obtained in good yield (56−67%) from the reaction of **2** with the corresponding $LnCl_3$ at 65 °C in molar ratios of 3:1 in dry THF. Similarly, the mixed coordinated complex {2,3-($SiMe_3$)$_2$-1-[4,5-(μ-H)-(*nido*-2-Me-3-($SiMe_3$)-2,3-$C_2B_4H_5$)]-1-Gd(η^5-2,3-$C_2B_4H_4$)}$_2$·3(THF) (**25**) was obtained by reacting compound **9** with **2**. To investigate the importance of the halide in these reactions, (η^5-Cp)$LnCl_2$ (Ln = Tb, Dy, Er) with **1** in a 1:2 molar ratio produced lanthanacarborane complexes [1-(η^5-C_5H_5)-2,3-($SiMe_3$)$_2$-1-Ln(η^5-2,3-$C_2B_4H_4$)]$_2$·*n*(THF) (**26**, Ln = Tb, *n* = 2; **27**, Ln = Dy, *n* = 2; **28**, Ln = Er, *n* = 3) as crystalline solids in 77−82% isolated yields. On the other hand, the reactions of (η^5-Cp)$_2$ErCl and (η^8-C_8H_8)GdCl with **1** in 1:1 molar ratios did not produce the half-sandwich lanthanacarboranes, but rather gave the *exo*-polyhedral products {*exo*-(η^5-C_5H_5)$_2$Er[4,5-(μ-H)-2,3-($SiMe_3$)$_2$-2,3-$C_2B_4H_4$]}·(THF) (**29**) and {*exo*-(η^8-C_8H_8)Gd[4,5-(μ-H)-2,3-($SiMe_3$)$_2$-2,3-$C_2B_4H_4$]·2(THF) (**30**) as crystalline solids in 76% and 73% isolated yield, respectively. All compounds were characterized by IR spectroscopy and elemental analysis, whereas compounds **3**, **7**−**9**, **10**−**16**, **18**−**22**, **29**, and **30** were characterized by single-crystal X-ray diffraction studies. The diamagnetic compounds **3**, **4**, and **16** were additionally characterized by ^{1}H, ^{13}C, and ^{11}B NMR spectroscopy.

Introduction

The systematic study of the f-block metallacarboranes began about 17 years ago with the report of the syntheses and structures of *closo*-3-Yb(DMF)$_4$-1,2-$C_2B_9H_{11}$ and [3,3′-(THF)$_2$-*commo*-3,3′-Sm($C_2B_9H_{11}$)$_2$]$^{2-}$, although the 5f complex [U($C_2B_9H_{11}$)$_2$-Cl_2]$^{2-}$ had been reported 11 years earlier.[1,2] Most of the initial studies involved the reaction of the respective lanthanide halide (LnX_2 or LnX_3) with the larger cage dianions *nido*-[$R_2C_2B_9H_9$]$^{2-}$ and *nido*-[$R_2C_2B_{10}H_{10}$]$^{2-}$. The products are diverse, ranging from half- to full-sandwich to *exo*-polyhedral metallacarboranes, depending on the nature of the R group on the carborane, the lanthanide and its charge, and the starting stoichiometry used in the reactions.[3] There has been added emphasis on synthesizing the half-sandwich halolanthanacarboranes, since the reactive Ln−Cl bond can lead to a variety of other mixed lanthanacar-

---

* To whom correspondence should be addressed. E-mail: hosmane@niu.edu.

[†] Northern Illinois University.

[‡] Southern Methodist University.

[1] Fronczek, F. R.; Halstead, G. W.; Raymond, K. N. *J. Am. Chem. Soc.* **1977**, *99*, 1769−1775.

[2] Manning, M. J.; Knobler, C. B.; Hawthorne, M. F. *J. Am. Chem. Soc.* **1988**, *110*, 4458−4459.

[3] For recent reviews see: (a) Saxena, A. K.; Hosmane, N. S. *Chem. Rev.* **1993**, *93*, 1081−1124. (b) Xie, Z.; *Coord. Chem. Rev.* **2002**, *231*, 23−46.

10.1021/om060268k CCC: $33.50

boranes.[4] The chemistry of the smaller cage, C_2B_4, based lanthanacarboranes is even more complex. Their initial report was on the synthesis of the trinuclear cluster $\{[\eta^5\text{-1-Gd-2,3-(SiMe}_3)_2\text{-2,3-C}_2B_4H_4]_3[(\mu_2\text{-1-Li-2,3-(SiMe}_3)_2\text{-2,3-C}_2B_4H_4)_3(\mu_3\text{-OMe})][\mu_2\text{-Li(THF)}]_3(\mu_3\text{-O})\}$, which was the unexpected product of the reaction of $GdCl_3$ with the THF-solvated dilithium compound of $[2,3\text{-(SiMe}_3)_2\text{-2,3-C}_2B_4H_4]^{2-}$.[5a] Rather than being an isolated incident, this proved to be a general reaction, and a number of similar trinuclear lanthanacarborane clusters (Ln = Nd, Sm, Gd, Tb, Dy, Ho) have been synthesized and structurally characterized.[5b,c] In all cases, the methoxide and oxide ions were believed to come from the degradation of the THF molecules. Support for this contention came from the observation that when TMEDA was substituted for THF, a 1:2 molar ratio reaction of $LnCl_3$ with carborane produced the expected chlorolanthanacarboranes, $[\{\eta^5\text{-2,3-(Me}_3\text{Si)}_2C_2B_4H_4\}_2\text{LnCl}_2]\text{Li}_3\text{(TMEDA)}_4]$ (Ln = Sm, Gd, Dy, Ho, Er).[6] The propensity to degrade THF seems to be present only in the 2,3-C_2B_4 (carbons adjacent) cage system. There is an isomeric cage in which the two carbons on the C_2B_3 bonding face are separated by a boron atom to give the 2,4-C_2B_4 or carbons-apart isomer. Reactions of $LnCl_3$ (Ln = Nd, Gd, Dy, Ho, Er, Tb, Lu) with *closo*-*exo*-5,6-Na-$(\text{THF})_2$-1-Na$(\text{THF})_2$-2,4-$(\text{SiMe}_3)_2$-2,4-$C_2B_4H_4$ in 1:2 molar ratios produced only the full-sandwich lanthanacarboranes [1,1′-*commo*-Ln$(2,4\text{-(SiMe}_3)_2\text{-2,4-C}_2B_2H_4)_2]^-$ in good yields.[7] A 1:1 molar ratio of $GdCl_3$ and the carborane ligand gave the dimeric half-sandwich gadolinacarborane $\{1,1\text{-Cl}_2[\mu,\mu'\text{-Na(TMEDA)}]$-1-(THF)-2,4-$(\text{SiMe}_3)_2$-*closo*-1-Gd-2,4-$C_2B_4H_4\}_2$ in 88% yield.[8] Other than its implied reaction with a second equivalent of *closo*-*exo*-5,6-Na$(\text{THF})_2$-1-Na$(\text{THF})_2$-2,4-$(\text{SiMe}_3)_2$-2,4-$C_2B_4H_4$ to form the full-sandwich gadolinacarborane, the reactivity of the Gd−Cl bond was not investigated. Indeed, most of the studies of the Ln−X carboranes have involved their reactions with additional *nido*-carborane anions, and very few other possibilities in their reaction chemistry have been explored.[4a,9] To investigate the utility of the halolanthanacarboranes as useful precursors in the syntheses of potentially useful organometallic compounds, a direct synthesis route to the simple half-sandwich halometallacarboranes is needed. While this may prove possible in the large cage and the small-cage "carbons-apart" systems, there is as yet no reliable synthetic method described for the "carbons-adjacent" 1,2,3-$(\text{LnX})C_2B_4$ complexes. With this in mind, we initiated an investigation of a simple, direct route to the synthesis of such complexes. The initial results of this investigation were described in a preliminary communication.[10] Herein, we report a more extensive application of the method, along with the structural characterizations of the products. In addition, the limitations of the method were investigated using CpLnCl_2, Cp_2-LnCl, and $(C_8H_8)\text{LnCl}$ as well as LnX_3 (X = Cl or Br) as lanthanide sources.

Experimental Section

Materials. Benzene, toluene, tetrahydrofuran (THF), and *n*-hexane were dried over NaH or Na/benzophenone and doubly distilled before use. The synthesis of *nido*-1-Na(THF)-2,3-$(\text{SiMe}_3)_2$-2,3-$C_2B_4H_5$ (**1**) and *nido*-1-Na(THF)-2-Me-3-(SiMe_3)-2,3-$C_2B_4H_5$- (**2**) (THF = C_4H_8O) followed the published procedure.[11] YCl_3, $LaBr_3$, $CeBr_3$, $PrCl_3$, $NdCl_3$, $SmBr_3$, $GdCl_3$, $TbCl_3$, $DyCl_3$, $HoCl_3$, $ErCl_3$, $TmCl_3$, $YbCl_3$, and $LuCl_3$, purchased from Aldrich, were degassed in vacuo at 130 °C for 24 h prior to use. Compounds of $(\eta^5\text{-Cp})\text{LnCl}_2$,[12] $(\eta^5\text{-Cp})_2\text{LnCl}$,[13] and $(\eta^8\text{-C}_8H_8)\text{LnCl}$[14] were prepared by literature methods.

Spectroscopic Procedures. Proton, boron-11, and carbon-13 NMR spectra were recorded on a Bruker Fourier transform multinuclear NMR spectrometer at 200, 64.2, and 50.3 MHz, respectively. Infrared spectra were recorded on a Perkin-Elmer Model 1600 FT-IR spectrophotometer or a Nicolet Magna 550 FT-IR spectrophotometer. Elemental analyses were determined in house at Northern Illinois University using a Perkin-Elmer 2400 CHN elemental analyzer.

Synthetic Procedures. All experiments were carried out in 100 mL Pyrex glass round-bottom flasks, equipped with magnetic stirring bars and high-vacuum Teflon valves. After their initial purifications, nonvolatile substances were manipulated in either a drybox or a glovebag, under an atmosphere of dry nitrogen. All known compounds among the products were identified by comparing their IR and/or ^{1}H NMR spectra with those of authentic samples.

Synthesis of $[2,3\text{-(SiMe}_3)_2\text{-1-X-1-(THF)}_m\text{-1-Ln}(\eta^5\text{-2,3-C}_2B_4H_4)]_2\cdot n\text{(THF)}$ (3, Ln = Y, X = Cl, *m* = 2, *n* = 2; 4, Ln = La, X = Br; *m* = 1, *n* = 0; 5, Ln = Ce, X = Br; *m* = 1, *n* = 0; 6, Ln = Pr, X = Br; *m* = 2, *n* = 1; 7, Ln = Nd; X = Cl, *m* = 2, *n* = 2; 8, Ln = Sm; X = Br, *m* = 2, *n* = 1; 9, Ln = Gd; X = Cl, *m* = 2, *n* = 1; 10, Ln = Tb, X = Cl, *m* = 2, *n* = 1; 11, Ln = Dy, X = Cl, *m* = 2, *n* = 1; 12, Ln = Ho, X = Cl, *m* = 2, *n* = 1; 13, Ln = Er, X = Cl, *m* = 2, *n* = 1; 14, Ln = Tm, X = Cl, *m* = 2, *n* = 1; 15, Ln = Yb, X = Cl, *m* = 2, *n* = 1; 16, Ln = Lu X = Cl, *m* = 2, *n* = 1). Except for the quantities used, the procedures in the syntheses of compounds **3**−**16** were identical. Therefore, only a typical synthesis will be described; the details of quantities used, product yields, and certain physical properties of **3**−**16** are summarized in Table 1.

A previously weighed sample of *nido*-1-Na(THF)-2,3-$(\text{SiMe}_3)_2$-2,3-$C_2B_4H_5$ (**1**) was mixed with anhydrous $LnCl_3$ (or $SmBr_3$, $CeBr_3$, or $LaBr_3$) in a molar ratio of 2:1, in about 30−40 mL of dry THF, and stirred at −76 °C for 2−3 h. The reaction mixture was slowly warmed to room temperature, then heated to 60 °C and stirred for an additional 24 h. During this period the solution became turbid and turned dark brown. The heterogeneous product mixture was filtered through a frit, and the residue was washed repeatedly with anhydrous benzene. The solid that remained on the frit after several washings was identified as NaCl (or NaBr when $LnBr_3$ was used; not measured) and was discarded. Removal of volatiles from the clear solution gave a solid that was later recrystallized from THF solvent to collect air-sensitive crystals of the particular color (see Table 1), identified as the dimers $[2,3\text{-(SiMe}_3)_2\text{-1-X-1-(THF)}_m\text{-1-Ln}(\eta^5\text{-2,3-C}_2B_4H_4)]_2\cdot\text{(THF)}_n$ (**3**, Ln = Y, X = Cl, *m* = 2, *n* = 1; **4**, Ln = La, X = Br; *m* = 1, *n* = 0; **5**, Ln = Ce, X = Br; *m* = 1, *n* = 0; **6**, Ln = Pr, X = Br; *m* = 2, *n* = 0; **7**, Ln = Nd; X = Cl,

---

[4] Ciu, K.-y.; Zhang, Z.; Mak, T. C. W.; Xie, Z. *J. Orgnomet. Chem.* **2000**, *614/615*, 107.

[5] (a) Oki, A. R.; Zhang, H.; Hosmane, N. S. *Angew. Chem., Int. Ed. Engl.* **1992**, *31*, 432. (b) Zhang, H.; Oki, A. R. Wang, Y.; Maguire, J. A.; Hosmane, N. S. *Acta Crystallogr.* **1995**, *C51*, 635. (c) Hosmane, N. S.; Wang, Y.; Oki, A. R.; Zhang, H.; Maguire, J. A. *Organometallics* **1996**, *15*, 626.

[6] Hosmane, N. S.; Wang, Y.; Zhang, H.; Maguire, J. A.; McInnis, M.; Gray, T. G.; Collins, J. D. *Organometallics* **1996**, *15*, 1006.

[7] Wang, J.; Li, S.; Zheng, C.; Maguire, J. A.; Sarkar, B.; Kaim, W.; Hosmane, N. S. *Organometallics* **2003**, *22* (21), 4334−4342.

[8] Hosmane, N. S.; Li. S.; Zheng, C.; Maguire, J. A. *Inorg. Chem. Commun.* **2001**, *4*, 104.

[9] Hosmane, N. S.; Wang, Y.; Zhang, H.; Oki, A. R.; Maguire, J. A.; Waldhor, E.; Kain, W.; Binder, H.; Kremer, R. K. *Organometallics* **1995**, *14*, 1101−1103.

[10] Wang, J.; Zheng, C.; Li, A.; Allard, C. L.; Smith, J. L.; Arikatla, G.; Maguire, J. A.; Hosmane, N. S. **2004**, *7*, 1078−1081.

[11] Hosmane, N. S.; Saxena, A. K.; Barreto, R. D.; Zhang, H.; Maguire, J. A.; Jia, L.; Wang, Y.; Oki, A. R.; Grover, K. V.; Whitten, S. J.; Dawson, K.; Tolle, M. A.; Sirriwardane, U.; Demissie, T.; Fagner, J. S. *Organometallics* **1993**, *12*, 3001−3014.

[12] Manastyrskyj, S.; Maginn, R. E.; Dubeck, M. *Inorg. Chem.* **1963**, *2* (5), 904−905. (b) Hou, Z.; Wakatsuki, Y. *Sci. Synth.* **2003**, *2*, 849−942.

[13] Schumann, H.; Lauke, H.; Hahn, E.; Heeg, M. J. *Organometallics* **1985**, *4* (2), 321−324.

[14] Wayda, A. L. *Inorg. Synth.* **1990**, *27*, 150−154. (b) Burton, N. C.; Cloke, F. G. N.; Hitchcock, P. B.; De Lemos, H. C.; Sameh, A. A. *J. Chem. Soc., Chem. Commun.* **1989**, *19*, 1462−1464.

Table 1. Preparation and Selected Physical Properties of 3-21

compd	ligand (g, mmol)	LnX_3 (g, mmol)	color	Mp (°C) (dec)	product (g, mmol)	recovered carborane (g, mmol)	yield (%)
3	1.26, 4.00[a]	YCl_3 0.39, 2.00	colorless	80−81	0.83, 0.80[b]	0.43, 1.97	80
4	0.60, 1.92[a]	$LaBr_3$ 0.50, 0.96	colorless	>250	0.43, 0.42[c]	0.20, 0.93	88
5	0.60, 1.92[a]	$CeBr_3$ 0.50, 0.96	yellow	>250	0.45, 0.44[c]	0.21, 0.96	92
6	0.82, 2.62[a]	$PrBr_3$ 0.50, 1.31	light blue	78−80	0.66, 0.54[b]	0.30, 1.37	82
7	1.26, 4.00[a]	$NdCl_3$ 0.50, 2.00	blue	120−122	1.06, 0.92[b]	0.43, 1.94	92
8	0.83, 2.56[a]	$SmBr_3$ 0.50, 1.28	yellow	85−86	0.67, 0.53[b]	0.299, 1.36	83
9	1.19, 3.80[a]	$GdCl_3$ 0.50, 1.90	colorless	87−89	0.84, 0.71[b]	0.40, 1.82	75
10	1.18, 3.76[a]	$TbCl_3$ 0.50, 1.88	colorless	93−94	0.89, 0.75[b]	0.398, 1.81	80
11	1.17, 3.72[a]	$DyCl_3$ 0.50, 1.86	colorless	94−96	0.90, 0.76[b]	0.40, 1.84	82
12	1.15, 3.68[a]	$HoCl_3$ 0.50, 1.84	pink	89−90	0.84, 0.70[b]	0.44, 2.00	77
13	1.15, 3.66[a]	$ErCl_3$ 0.50, 1.83	pink	75−77	0.85, 0.71[b]	0.45, 2.05	78
14	1.14, 3.64[a]	$TmCl_3$ 0.50, 1.82	colorless	80−81	0.86, 0.72[b]	0.43, 1.96	79
15	1.12, 3.58[a]	$YbCl_3$ 0.50, 1.79	red	104−105	0.80, 0.66[b]	0.46, 2.09	74
16	1.11, 3.56[a]	$LuCl_3$ 0.50, 1.78	colorless	132−133	0.82, 0.68[b]	0.44, 2.00	76
17	1.02, 4.00[d]	$NdCl_3$ 0.50, 2.00	blue	110−112	0.69, 0.70[e]	0.36, 2.23	72
18	0.95, 3.72[d]	$DyCl_3$ 0.50, 1.86	colorless	81−83	0.70, 0.70[e]	0.35, 2.17	75
19	0.94, 3.68[d]	$HoCl_3$ 0.50, 1.84	pink	71−73	0.70, 0.69[e]	0.36, 2.23	75
20	0.93, 3.66[d]	$ErCl_3$ 0.50, 1.83	pink	70−72	0.70, 0.70[e]	0.338, 2.09	76
21	0.91, 3.58[d]	$YbCl_3$ 0.50, 1.79	red	92−94	0.73, 0.72[e]	0.32, 1.98	80

[a] Ligand = *nido*-1-Na(C_4H_8O)-2,3-$(SiMe_3)_2$-2,3-$C_2B_4H_5$ (**1**). [b]Products = [2,3 -$(SiMe_3)_2$-1-X-1-Ln(η^5-2,3-$C_2B_4H_4$)]$_2$•5(THF). [c]Products = [2,3-$(SiMe_3)_2$-1-X-1-Ln(η^5-2,3-$C_2B_4H_4$)]$_2$•2 (THF). [d]Ligand = *nido*-1-Na(C_4H_8O)-2-Me-3-($SiMe_3$)-2,3-$C_2B_4H_5$ (**2**). [e]Products = [2-Me-3-$(SiMe_3)_2$-1-Cl-1-$(THF)_2$-1-Ln(η^5-2,3-$C_2B_4H_4$)]$_2$.

m = 2, n = 1; **8**, Ln = Sm; X = Br, m = 2, n = 1; **9**, Ln = Gd; X = Cl, m = 2, n = 1; **10**, Ln = Tb, X = Cl, m = 2, n = 1; **11**, Ln = Dy, X = Cl, m = 2, n = 1; **12**, Ln = Ho, X = Cl, m = 2, n = 1; **13**, Ln = Er, X = Cl, m = 2, n = 1; **14**, Ln = Tm, X = Cl, m = 2, n = 1; **15**, Ln = Yb, X = Cl, m = 2, n = 1; **16**, Ln = Lu X = Cl, m = 2, n = 1). The volatiles were fractionated through a 0 °C bath to collect essentially half the beginning carborane as the neutral *nido*-2,3-$(SiMe_3)_2$-2,3-$C_2B_4H_6$ (0 °C); THF and benzene were collected at −196 °C. The product yields and selected physical properties are presented in Table 1, while the analytical data are given in Table 2. The infrared spectral data, with selected assignments for **3**−**16**, are given in Table 3.

NMR data for complex **3**: ^1H NMR (d_8-THF, relative to external Me_4Si) δ 0.14, 0.07 [36 H, s (CH_3 in $SiMe_3$)], 1.74 (m, 20 H, C_4H_8O), 3.75 (m, 20 H, C_4H_8O); ^{13}C NMR (d_8-THF, relative to external Me_4Si) δ 0.8, 0.6 [CH_3 on $SiMe_3$], 22.6, 64.7 [C_4H_8O]; ^{11}B NMR (d_8-THF, relative to external BF_3•OEt_2) δ 11.9 [br, 1B, basal BH], −0.77 [d, 2B, basal BH, $^1J(^{11}B-^1H)$ = 130 Hz], −52.7 [d, 1B, apical BH, $^1J(^{11}B-^1H)$ = 175 Hz]. Complex **4**: ^1H NMR (d_8-THF, relative to external Me_4Si) δ 0.10 [18 H, s (CH_3 in $SiMe_3$)], 1.72 (4 H, s, br, C_4H_8O), 3.58 (4 H, s, br, C_4H_8O); ^{13}C NMR (d_8-THF, relative to external Me_4Si) δ 1.5 [q, CH_3 on $SiMe_3$, $^1J(^{13}C-^1H)$ = 118.2 Hz], 25.5, 67.6 [m, C_4H_8O]; ^{11}B NMR (d_8-THF, relative to external BF_3•OEt_2) δ 13.34 [br, 1B, basal BH], −1.15 [d, 2B, basal BH, $^1J(^{11}B-^1H)$ = 148 Hz], −51.80 [d, 1B, apical BH, $^1J(^{11}B\text{-}^1H)$ = 171 Hz]. Complex **16**: ^1H NMR (d_8-THF, relative to external Me_4Si) δ 0.20 [36 H, s (CH_3 in $SiMe_3$)], 1.73 (20H, s, br, C_4H_8O), 3.58 (20 H, s, br, C_4H_8O); ^{13}C NMR (d_8-THF, relative to external Me_4Si) δ 1.20 [q, CH_3 on $SiMe_3$, $^1J(^{13}C-^1H)$ = 118.0 Hz], 23.3, 65.7 [m, C_4H_8O]; ^{11}B NMR (d_8-THF, relative to external BF_3•OEt_2) δ 25.91 [br, 1B, basal BH], −1.01 [d, 2B, basal BH, $^1J(^{11}B-^1H)$ = 130 Hz], −52.71 [d, 1B, apical BH, $^1J(^{11}B-^1H)$ = 184 Hz].

Table 2. Analytical Data for Compounds 3−21

no.	compound formula	carbon		hydrogen	
		calcd	found	calcd	found
3	$(C_8H_{22}B_4ClSi_2Y)_2$•5(THF)	41.59	41.35	7.66	7.53
4	$(C_8H_{22}B_4BrSi_2La)_2$•2(THF)	28.40	28.39	5.76	6.02
5	$(C_8H_{22}B_4BrSi_2Ce)_2$•2(THF)	28.33	28.50	5.75	6.04
6	$(C_8H_{22}B_4BrSi_2Pr)_2$•5(THF)	34.94	34.66	6.84	6.74
7	$(C_8H_{22}B_4ClSi_2Nd)_2$•5(THF)	37.59	37.39	6.92	6.80
8	$(C_8H_{22}B_4BrSi_2Sm)_2$•5(THF)	34.41	34.56	6.74	6.51
9	$(C_8H_{22}B_4ClSi_2Gd)_2$•5(THF)	36.76	36.62	6.77	6.53
10	$(C_8H_{22}B_4ClSi_2Tb)_2$•5(THF)	36.66	36.48	6.75	6.56
11	$(C_8H_{22}B_4ClSi_2Dy)_2$•5(THF)	36.43	36.45	6.71	6.52
12	$(C_8H_{22}B_4ClSi_2Ho)_2$•5(THF)	36.29	36.54	6.68	6.98
13	$(C_8H_{22}B_4ClSi_2Er)_2$•5(THF)	36.14	36.21	6.66	6.48
14	$(C_8H_{22}B_4ClSi_2Tm)_2$•5(THF)	36.04	36.28	6.64	6.32
15	$(C_8H_{22}B_4ClSi_2Yb)_2$•5(THF)	35.80	35.55	6.59	6.37
16	$(C_8H_{22}B_4ClSi_2Lu)_2$•5(THF)	35.68	35.37	6.57	6.24
17	$[C_6H_{16}B_4Cl\ SiNd]_2$ •4(THF)	34.78	34.73	6.67	6.54
18	$[C_6H_{16}B_4Cl\ SiDy]_2$ •4(THF)	33.52	33.40	6.43	6.07
19	$[C_6H_{16}B_4Cl\ SiHo]_2$ •4(THF)	33.36	33.60	6.40	6.15
20	$[C_6H_{16}B_4Cl\ SiEr]_2$ •4(THF)	33.20	33.03	6.37	6.12
21	$[C_6H_{16}B_4Cl\ SiYb]_2$ •4(THF)	32.83	32.71	6.30	6.23

Synthesis of [2-Me-3-($SiMe_3$)-1-Cl-1-$(THF)_2$-1-Ln(η^5-2,3-$C_2B_4H_4$)]$_2$ (17, Ln = Nd; 18, Ln = Dy; 19, Ln = Ho; 20, Ln =

Table 3. Infrared Absorptions (cm^{-1}, KBr pellet)[a]

compd	IR spectra data
3	2958(vs), 2896(m), 2593(m), 2529(m), 2520(m), 2407(m), 2366(m), 1458(w), 1400(m), 1247(s), 1184(m), 1067(m), 1022(m), 1008(m), 834(vs), 754(m), 684(m), 631(m)
4	2970(vs), 2883(m), 2597(m), 2576(m), 1614(w), 1393(m), 1255(s), 1096(m), 1015(m), 850(vs), 830(m), 794(m)
5	2955(vs), 2894(m), 2853(m), 2582(m), 1619(w), 1404(w), 1260(s), 1096(m), 1025(m), 830(vs), 753(m), 676(m), 620(m)
6	2971(vs), 2889(m), 2587(s), 1619(w), 1455(w), 1393(m), 1255(s), 1091(m), 1015(m), 907(m), 856(vs), 830(m), 794(m), 661(m)
7	2970(vs), 2951(m), 2889(m), 2591(m), 2534(m), 2506(m), 2402(m), 2365(m), 1398(m), 1248(s), 1017(m), 840(vs), 750(m), 683(m), 630(m)
8	2959(vs), 2893(m), 2589(m), 2540(m), 2508(m), 2413(m), 2365(m), 1454(w), 1400(m), 1248(s), 1182(m), 1066(m), 1024(m), 838(vs), 754(m), 680(m), 629(m)
9	2953(vs), 2893(m), 2586(m), 2525(m), 2404(m), 2366(m), 1625(w), 1451(m), 1398(m), 1248(s), 1180(m), 1066(m), 1025(m), 1007(m), 833(vs), 755(m), 685(m), 626(m)
10	2959(vs), 2893(m), 2589(m), 2589(m), 2540(m), 2508(m), 2413(m), 2365(m), 1454(m), 1400(m), 1248(s), 1182(m), 1066(m), 1024(m), 914(m), 838(vs), 754(m), 680(m),629(m)
11	2968(vs), 2891(m), 2592(m), 2528(m), 2406(m), 2365(m), 1636(w), 1459(m), 1400(m), 1341(m), 1248(s), 1183(m), 1015(m), 921(m), 862(s), 754(m), 676(m), 631(m)
12	2959(vs), 2891(m), 2592(m), 2524(m), 2411(m), 2361(m), 1455(w), 1396(s), 1187(m), 1074(m), 1024(m), 834(s), 762(m), 680(m), 630(m)
13	2964(vs), 2895(m), 2591(m), 2531(m), 2412(m), 2362(m), 1397(m), 1246(s), 1184(m), 1068(m), 1021(m), 831(s), 752(m), 681(m), 631(m)
14	2966(vs), 2894(m), 2592(m), 2525(m), 2418(m), 2361(m), 1634(w), 1455(w), 1399(m), 1245(s), 1184(m), 1066(m), 1015(m), 912(m), 856(s), 835(m), 753(m), 682(m), 625(m)
15	2953(vs), 2888(m), 2871(m), 2590(m), 2541(m), 2522(m), 2413(m), 2362(m), 2338(m), 1401(w), 1250(s), 1181(m), 1118(m), 1014(m), 858(s), 835(m), 759(m), 684(m)
16	2986(vs), 2904(m), 2587(m), 2530(m), 2413(m), 2366(m), 1634(w), 1455(w), 1399(m), 1245(s), 1178(m), 1015(m), 922(m), 851(vs), 677(m)
17	2957(s), 2893(m), 2587(m), 2531(m), 2491(m), 1453(m), 1404(w), 1251(s), 1094(m), 1024(m), 836(vs), 759(m), 690(m), 628(m)
18	2978(s), 2950(m), 2989(s), 2533(s), 2491(s), 2402(m), 2350(m), 1449(m), 1343(w), 1243(s), 1091(m), 1036(s), 837(br, vs), 756(m), 684(m), 629(m)
19	2957(s), 2900(s), 2532(s), 2488(s), 2405(m), 2348(m), 2123(w), 1449(m), 1344(w), 1242(s), 1121(m), 1032(s), 846(br, vs), 757(m), 685(m), 630(m)
20	2955(s), 2894(s), 2532(s), 2490(s), 2401(m), 2350(m), 1450(m), 1397(w), 1241(s), 1034(s), 838(br, vs), 755(m), 686(m), 630(m)
21	2960(s), 2897(m), 2533(s), 2493(s), 2358(m), 1456(s), 1399(s), 1227(m), 1094(s), 837(vs), 630(s)

[a] Legend: v = very, s = strong or sharp, m = medium, w = weak, and br = broad.

Er; 21, Ln = Yb). Using the same procedure as described above, a previously weighed sample of *nido*-1-Na(THF)-2-Me-3-($SiMe_3$)-2,3-$C_2B_4H_5$ (**2**) was reacted with $LnCl_3$ (Ln = Nd, Dy, Ho, Er, Yb) in a molar ratio of 2:1 in anhydrous THF at 65 °C to give complexes of formula [2 -Me-3-($SiMe_3$)-1-Cl-1-$(THF)_2$-1-Ln(η^5-2,3-$C_2B_4H_4$)]$_2$ (**17**, Ln = Nd; **18**, Ln = Dy; **19**, Ln = Ho; **20**, Ln = Er; **21**, Ln = Yb).

The yields and analyses are shown in Tables 1 and 2, respectively. The infrared spectral data with selected assignments for these compounds are shown in Table 3.

Synthesis of {2-Me-3-($SiMe_3$)-1-[4,5-(μ-H)-nido-2-Me-3-($SiMe_3$)-2,3-$C_2B_4H_5$]-1-Nd(η^5-2,3-$C_2B_4H_4$)}$_2$·4(THF) (22). A 0.50 g (0.52 mmol) sample of previously prepared [2-Me-3-($SiMe_3$)-1-Cl-1-Nd-(η^5-2,3-$C_2B_4H_4$)]$_2$·4 (THF) (**17**) was dissolved in 20 mL of anhydrous THF. The resulting solution was stirred and cooled to −78 °C, and a THF solution of a previously weighed sample of *nido*-1-Na(THF)-2-Me-3-($SiMe_3$)-2,3-$C_2B_4H_5$ (**2**) (0.14 g, 0.55 mmol) was added dropwise. After complete addition, the reaction mixture was warmed slowly to room temperature and stirred at 65 °C overnight, during which time the reaction mixture turned bluish-brown. The mixture was cooled to room temperature and then was filtered through a glass frit to obtain a clear blue solution. Solvent from the filtrate was completely evaporated under vacuum, and the resulting solid residue was dissolved in anhydrous benzene. The mixture was filtered again to obtain a clear solution. After removal of the solvent from the filtrate, a solid residue, identified as {2-Me-3-($SiMe_3$)-1-[4,5-(μ-H)-*nido*-2-Me-3-($SiMe_3$)-2,3-$C_2B_4H_5$]-1-Nd(η^5-2,3-$C_2B_4H_4$)}$_2$·4(THF) (**22**) (0.55 g, 0.45 mmol), was isolated in 87% yield. Anal. Calcd (found) for [$C_{12}H_{33}B_8NdSi_2$]·2THF (**22**): C, 39.61 (39.41); H, 7.81 (7.64). IR (cm^{-1}, KBr pellet): 2554(s), 2476 (s), 2415 (m), 2350 (s) [ν(B−H)].

Synthesis of {2-Me-3-($SiMe_3$)-1-[4,5-(μ-H)-nido-2-Me-3-($SiMe_3$)-2,3-$C_2B_4H_5$]-1-Ho(η^5-2,3-$C_2B_4H_4$)}$_3$·8(THF) (23). The procedure for the synthesis of compound **23** was identical to that of **22**. Therefore, only the amounts and yields are given here. A 0.50 g (0.50 mmol) sample of the previously prepared [2-Me-3-($SiMe_3$)-1-Cl-1-Ho(η^5-2,3-$C_2B_4H_4$)]$_2$·4(THF) (**19**) was reacted with 0.13 g (0.51 mmol) of *nido*-1-Na(THF)-2-Me-3-($SiMe_3$)-2,3-$C_2B_4H_5$ (**2**) to give trimeric {2-Me-3-($SiMe_3$)-1-[4,5-(μ-H)-*nido*-2-Me-3-($SiMe_3$)-2,3-$C_2B_4H_5$]-1-Ho(η^5-2,3-$C_2B_4H_4$)}$_3$·8(THF) (**23**) (0.55 g, 0.27 mmol; yield 54%). Anal. Calcd (found) for [$C_{12}H_{33}B_8HoSi_2$]$_3$·8THF (**23**): C, 40.36 (40.50); H, 7.72 (7.90). IR (cm^{-1}, KBr pellet): 2557 (s), 2515 (s), 2482 (s), 2450 (s) [ν(B−H)].

Synthesis of {2-Me-3-($SiMe_3$)-1-[4,5-(μ-H)-nido-2-Me-3-($SiMe_3$)-2,3-$C_2B_4H_4$]-1-Er(η^5-2,3-$C_2B_4H_4$)}$_2$·(THF) (24). The procedure for the synthesis of compound **24** was identical to that of **22**. A 0.50 g (0.50 mmol) sample of the previously prepared [2-Me-3-($SiMe_3$)-1-Cl-1-Er(η^5-2,3-$C_2B_4H_4$)]$_2$·4(THF) (**20**) was reacted with a 0.13 g (0.51 mmol) sample of *nido*-1-Na(THF)-2-Me-3-($SiMe_3$)-2,3-$C_2B_4H_5$ (**2**) to give the solid product {2-Me-3-($SiMe_3$)-1-[4,5-(μ-

H)-*nido*-2-Me-3-($SiMe_3$)-2,3-$C_2B_4H_5$]-1-Er(η^5-2,3-$C_2B_4H_4$)}$_2$·(THF) (**24**) (0.45 g, 0.43 mmol; yield 86%). Anal. Calcd (found) for [$C_{12}H_{33}B_8ErSi_2$]$_2$·THF (**24**): C, 32.16 (32.59); H, 7.04 (6.93). IR (cm^{-1}, KBr pellet): 2532 (s), 2490 (s), 2410 (m), 2355 (s) [ν(B−H)].

One-Pot Synthesis of {2-Me-3-($SiMe_3$)-1-[4,5-(μ-H)-nido-2-Me-3-($SiMe_3$)-2,3-$C_2B_4H_5$]-1-Nd(η^5-2,3-$C_2B_4H_4$)}$_2$·4(THF) (22). A 0.50 g (2.00 mmol) sample of $NdCl_3$ was mixed with 20 mL of anhydrous THF, and the resulting mixture was stirred overnight. The mixture was cooled to −78 °C, and to this was added dropwise a previously weighed sample of *nido*-1-Na(THF)-2-Me-3-($SiMe_3$)-2,3-$C_2B_4H_5$ (**2**) (1.54 g, 6.05 mmol). After complete addition, the reaction mixture was warmed slowly to room temperature and stirred at 65 °C overnight, during which time the reaction mixture turned bluish-brown. The reaction mixture was cooled to room temperature and filtered through a glass frit to obtain a clear blue solution. Solvent was removed from the filtrate in vacuo, and the remaining solid was extracted with anhydrous benzene. The resulting heterogeneous mixtures were combined and filtered again to obtain a clear solution. After removal of the solvent from the filtrate, a solid product, identified as {2-Me-3-($SiMe_3$)-1-[4,5-(μ-H)-*nido*-2-Me-3-($SiMe_3$)-2,3-$C_2B_4H_5$]-1-Nd(η^5-2,3-$C_2B_4H_4$)}$_2$·4(THF), **22** (0.69 g, 0.56 mmol), was obtained in 56% yield.

One-Pot Syntheses of Trimeric {2-Me-3-($SiMe_3$)-1-[4,5-(μ-H)-nido-2-Me-3-($SiMe_3$)-2,3-$C_2B_4H_5$]-1-Ho(η^5-2,3-$C_2B_4H_4$)}$_3$·8-(THF) (23) and Dimeric {2-Me-3-($SiMe_3$)-1-[4,5-(μ-H)-nido-2-Me-3-($SiMe_3$)-2,3-$C_2B_4H_5$]-1-Er(η^5-2,3-$C_2B_4H_4$)}$_2$·(THF) (24). Except for the quantities used, the syntheses of compounds **23** and **24** were identical to that of **22**. Therefore, only the quantities and yields are presented.

23. A 0.50 g (1.84 mmol) sample of $HoCl_3$ was reacted with **2** (1.40 g, 5.53 mmol) in anhydrous THF to give {2-Me-3-($SiMe_3$)-1-[4,5-(μ-H)-*nido*-2-Me-3-($SiMe_3$)-2,3-$C_2B_4H_5$]-1-Ho(η^5-2,3-$C_2B_4H_4$)}$_3$·8(THF), **23** (0.83 g, 0.41 mmol; yield 67%).

24. A 0.50 g (1.83 mmol) sample of $ErCl_3$ was reacted with **2** (1.44 g, 5.66 mmol) in anhydrous THF to give{2-Me-3-($SiMe_3$)-1-[4,5-(μ-H)-*nido*-2-Me-3-($SiMe_3$)-2,3-$C_2B_4H_5$]-1-Er(η^5-2,3-$C_2B_4H_4$)}$_2$· (THF), **24** (0.61 g, 0.57 mmol; yield 63%).

Synthesis of Mixed-Ligand {2,3-($SiMe_3$)$_2$-1-[4,5-(μ-H)-nido-2-Me-3-($SiMe_3$)-2,3-$C_2B_4H_5$]-1-Gd(η^5-2,3-$C_2B_4H_4$)}$_2$·3(THF) (25). Using the same procedure described above, the previously prepared half-sandwich complex **9** (0.50 g, 0.42 mmol) reacted with **2** (0.22 g, 0.42 mmol) to give {2,3-($SiMe_3$)$_2$-1-[4,5-(μ-H)-*nido*-2-Me-3-($SiMe_3$)-2,3-$C_2B_4H_5$]-1-Gd(η^5-2,3-$C_2B_4H_4$)}$_2$·3(THF), **25** (0.45 g, 0.35 mmol; yield 83%). Anal. Calcd (found) for ($C_{14}H_{39}B_8Si_3Gd$)$_2$·3(THF) (**25**): C, 37.32 (37.36); H, 7.99 (7.76). IR (cm^{-1}, KBr pellet): 2590 (m), 2529 (s, br), 2408 (s), 2365 (s) [ν(B−H)].

Synthesis of [1-(η^5-C_5H_5)-2,3-($SiMe_3$)$_2$-1-Tb(η^5-2,3-$C_2B_4H_4$)]·(THF) (26). A 0.32 g (1.09 mmol) sample of (η^5-Cp)$TbCl_2$ was dissolved in 20 mL of THF, the resulting solution was then cooled to −76 °, and then a 10 mL THF solution of *nido*-1-Na(C_4H_8O)-2,3-($SiMe_3$)$_2$-2,3-$C_2B_4H_5$ (**1**) (0.71 g, 2.13 mmol) was added dropwise. After the addition was finished, the reaction mixture was slowly warmed to room temperature and then stirred at 65 °C overnight, during which time the reaction mixture turned turbid and was filtered thought a glass frit to obtain a light yellow, clear solution. After removal of the solvent from the filtrate, the resulting solid was washed three times with hexanes (15 mL each) and was then recrystallized in THF/hexanes (1:3 v/v) to give a colorless crystalline compound, which was later identified as [1-(η^5-C_5H_5)-2,3-($SiMe_3$)$_2$-1-Tb(η^5-2,3-$C_2B_4H_4$)]·THF (**26**) (0.43 g, 0.84 mmol; yield 77%). Anal. Calcd (found) for ($C_{13}H_{27}B_4Si_2Tb$)·(THF) (**26**): C, 39.74 (39.52); H, 6.87 (6.61). IR (cm^{-1}, KBr pellet): 2548 (m), 2512 (s), 2485 (s) [ν(B−H)].

Synthesis of [1-(η^5-C_5H_5)-2,3-($SiMe_3$)$_2$-1-Dy(η^5-2,3-$C_2B_4H_4$)]·(THF) (27). In a procedure identical to that employed for compound **26** above, a 0.37 g (1.24 mmol) sample of (η^5-Cp)$DyCl_2$ was reacted with **1** (0.78 g, 2.50 mmol) to give [1-(η^5-C_5H_5)-2,3-($SiMe_3$)$_2$-1-Dy(η^5-2,3-$C_2B_4H_4$)]·THF (**27**) (0.50 g, 0.97 mmol; yield 78%). Anal. Calcd (found) for ($C_{13}H_{27}B_4Si_2Dy$)·(THF) (**27**): C, 39.47 (39.06); H, 6.82 (6.71). IR (cm^{-1}, KBr pellet): 2546 (m), 2510 (s), 2483 (s), 2356 (w), 2305 (m) [ν(B−H)].

Synthesis of [1-(η^5-C_5H_5)-2,3-($SiMe_3$)$_2$-1-Er(η^5-2,3-$C_2B_4H_4$)]$_2$·3(THF) (28). In a procedure identical to that employed for compound **26** above, a 0.42 g (1.39 mmol) sample of (η^5-Cp)$ErCl_2$ was reacted with **1** (0.87 g, 2.80 mmol) to give [1-(η^5-C_5H_5)-2,3-($SiMe_3$)$_2$-1-Er(η^5-2,3-$C_2B_4H_4$)]$_2$·3(THF) (**28**) (0.63 g, 0.57 mmol; yield 82%). Anal. Calcd (found) for ($C_{13}H_{27}B_4Si_2Er$)$_2$·3(THF) (**28**): C, 40.88 (40.56); H, 7.04 (7.33). IR (cm^{-1}, KBr pellet): 2550 (m), 2512 (s), 2485 (s), 2357 (w), 2306 (m) [ν(B−H)].

Synthesis of {exo-(η^5-C_5H_5)$_2$Er[4,5-(μ_2-H)-2,3-($SiMe_3$)$_2$-2,3-$C_2B_4H_5$]}·(THF) (29). A 0.45 g (1.35 mmol) sample of (η^5-Cp)$_2$-ErCl was dissolved in 20 mL of THF, cooled to −76 °C, and then 10 mL of a THF solution of *nido*-1-Na(C_4H_8O)-2,3-($SiMe_3$)$_2$-2,3-$C_2B_4H_5$ (**1**) (0.43 g, 1.35 mmol) was added dropwise in an inert atmosphere. The resulting mixture was slowly warmed to room temperature and then stirred at 65 °C overnight, during which time the reaction mixture turned turbid and was then filtered to obtain a clear solution. After complete removal of the solvent from the filtrate, the remaining solid was recrystallized from a THF and hexanes mixture (THF/hexeanes, 1:3) to give a light pink crystalline compound, which was identified as {(η^5-C_5H_5)$_2$Er[4,5-(μ_2-H)-2,3-($SiMe_3$)$_2$-2,3-$C_2B_4H_5$]}·THF, **29** (0.60 g, 1.03 mmol; yield 76%). Anal. Calcd (found) for ($C_{18}H_{33}B_4Si_2Er$)·(THF) (**29**): C, 45.00 (45.32); H, 6.87 (6.78).

Synthesis of {*exo*-(η^8-C_8H_8)Gd[4,5-(μ_2-H)-2,3-($SiMe_3$)$_2$-2,3-$C_2B_4H_5$]}·2(THF) (30). To a previously prepared THF solution of (η^8-C_8H_8)GdCl (0.5 g, 1.68 mmol) was added dropwise a 10 mL THF solution of *nido*-1-Na(C_4H_8O)-2,3-($SiMe_3$)$_2$-2,3-$C_2B_4H_5$ (**1**) (0.53 g, 1.71 mmol) at −76 °C. After the addition, the reaction mixture was slowly warmed to room temperature and then stirred at 65 °C overnight, during which time the reaction mixture turn turbid and was filtered through a glass frit to obtain a light yellow, clear solution. After removal of the solvent from the filtrate, the solid residue in the flask was washed three times with hexanes (15 mL each) and then recrystallized in THF/hexanes (1:3 v/v) to isolate a colorless crystalline solid, identified as {(η^8-C_8H_8)Gd[4,5-(μ_2-H)-2,3-($SiMe_3$)$_2$-2,3-$C_2B_4H_5$]}·2(THF) (**30**) (0.76 g, 1.22 mmol; mp 120−1 °C (dec)) in 73% yield. Anal. Calcd (found) for ($C_{16}H_{31}B_4$-Si_2Gd)·2(THF) (**30**): C, 46.32 (46.37); H, 7.29 (7.56). IR (cm^{-1}, KBr pellet) 2571 (s), 2537 (s, br), 2456 (s) [ν(B−H)].

X-ray Analyses of 3, 7−16, 18−21, 22, 29, and 30. X-ray quality crystals of **3**, **7−16**, and **18−21** were grown from a THF/*n*-hexane (60/40, v/v) solution by slow evaporation. Good quality crystals of **22** were obtained from a THF/benzene/*n*-hexane (1:2:7, v/v/v) mixture, while crystals of **29** and **30** were grown from THF/hexanes (40/60, v/v) solutions. The crystals were mounted on a Bruker SMART CCD PLATFORM diffractometer, under a low-temperature nitrogen stream. The pertinent crystallographic data for **3**, **7−16**, and **18−21** are summarized in Table 4, while crystallographic data for **22**, **29**, and **30** are listed in Table 5. Compounds **3**, **7−10** and **12−15** were found to be isostructural, and their space groups were uniquely determined from systematic absences as $P2_1/n$. Similar measurements on **18−21** and **29** were also consistent with the space group $P2_1/n$. Compound **22** was found to crystallize in the $C2/c$ space group, and compound **30** was determined as $P\bar{1}$. Intensity data for **9**, **11**, **15**, **18**, **21**, and **29** were collected at 203 K, for **13**, **16**, **19**, and **30**, data were collected at 213 K, and for compounds of **3**, **7**, **10**, **12**, **14**, and **20** the intensity data were collected at 208 K. Because of the instability of compound **22**, the intensity data for this compound were collected at 173 K. For each compound, 50 initial frames were repeated at the end of the collection for purposes of decay monitoring. No significant decays were observed for the compounds. All data considered as

Table 4. Crystallographic Data[a] for Complexes 3, 7−16, and 18−21 (all fw's reported as monomer formula weights)

	3	**7**	**8**	**9**	**10**
formula	$C_{20}H_{46}B_4ClO_3Si_2Y$	$C_{20}H_{46}B_4ClNdO_3Si_2$	$C_{20}H_{46}B_4BrO_3Si_2Sm$	$C_{20}H_{46}B_4ClGdO_3Si_2$	$C_{20}H_{46}$ $B_4ClO_3Si_2Tb$
fw	558.35	613.68	664.25	626.69	628.36
cryst syst	monoclinic	monoclinic	monoclinic	monoclinic	monoclinic
space group	$P2_1/n$	$P2_1/n$	$P2_1/n$	$P2_1/n$	$P2_1/n$
a, Å	15.956(3)	15.924(3)	15.848(3)	15.946(4)	15.966(3)
b, Å	11.396(2)	11.540(2)	11.644(2)	11.442(3)	11.432(2)
c, Å	16.968(4)	17.016(3)	16.909(3)	16.990(4)	17.002(4)
β, deg	108.887(3)	109.250(3)	102.038(6)	108.977(4)	108.972(3)
V, Å^3	2919.2(11)	2952.0(9)	108.869(3)	2931.7(11)	2934.6(11)
Z	4	4	4	4	4
D_{calcd}, g cm^{-3}	1.270	1.381	1.494	1.420	1.422
abs coeff, mm^{-1}	2.190	1.949	3.441	2.453	2.601
scan angles in θ; min., max.	1.52, 25.00	2.14, 25.00	1.53, 21.00	1.52, 25.00	1.52, 25.00
T, K	208(2)	208(2)	173(2)	203(2)	208(2)
no. of data collected	17 584	19 909	11 657	10 343	18 372
unique reflctns	4981	5144	3116	5053	5088
no. of params refined	327	327	327	327	327
GOF	1.322	1.650	1.539	1.523	1.541
R_1 [$I > 2\sigma(I)$]	0.0704	0.0768	0.0955	0.0418	0.0496
wR_2 [$I>2\sigma(I)$]	0.1324	0.1470	0.1902	0.0857	0.1073

	11	**12**	**13**	**14**	**15**
formula	$C_{20}H_{46}B_4ClDyO_3Si_2$	$C_{20}H_{46}B_4ClHoO_3Si_2$	$C_{20}H_{46}B_4ClErO_3Si_2$	$C_{20}H_{46}B_4ClO_3Si_2Tm$	$C_{20}H_{46}B_4ClO_3Si_2Yb$
fw	631.94	634.37	636.70	638.37	642.48
cryst syst	monoclinic	monoclinic	monoclinic	monoclinic	monoclinic
space group	$P2_1/c$	$P2_1/n$	$P2_1/n$	$P2_1/n$	$P2_1/n$
a, Å	15.951(3)	15.878(3)	15.948(3)	15.942(3)	15.952(2)
b, Å	11.403(2)	11.338(2)	11.377(2)	11.358(2)	11.352(2)
c, Å	16.982(3)	16.909(4)	16.973(3)	16.952(3)	16.954(3)
β, deg	108.928(3)	108.957(3)	108.959(3)	108.892(3)	108.911(2)
V, Å^3	2921.9(10)	2878.9(10)	2912.5(9)	2904.1(9)	2904.6(7)
Z	4	4	4	4	4
D_{calcd}, g cm^{-3}	1.437	1.464	1.452	1.460	1.469
abs coeff, mm^{-1}	2.749	2.943	3.074	3.248	3.413
scan angles in θ; min, max	1.52, 25.00	1.53, 25.00	1.52, 25.00	2.13, 25.00	1.52, 25.00
T, K	203(2)	208(2)	213(2)	208(2)	203(2)
no. of data collected	19 792	18 909	18 841	19 421	20 379
unique reflctns	5140	4997	5136	5100	5120
no. of params refined	327	327	327	327	327
GOF	1.456	1.426	1.434	1.551	1.802
R_1 [$I > 2\sigma(I)$]	0.0393	0.0617	0.0323	0.0392	0.0630
wR_2 [$I > 2\sigma(I)$]	0.0809	0.1439	0.0672	0.0805	0.1033

	16	**18**	**19**	**20**	**21**
formula	$C_{20}H_{46}B_4ClLuO_3Si_2$	$C_{14}H_{32}B_4Cl$ DyO_2Si	$C_{14}H_{32}B_4ClHoO_2Si$	$C_{14}H_{32}B_4ClErO_2Si$	$C_{14}H_{32}B_4ClO_2SiYb$
fw	644.41	501.68	504.11	506.44	512.22
cryst syst	monoclinic	monoclinic	monoclinic	monoclinic	monoclinic
space group	$P2_1/n$	$P2_1/n$	$P2_1/n$	$P2_1/n$	$P2_1/n$
a, Å	15.958(5)	9.626(2)	9.615(1)	9.627(2)	9.5975(9)
b, Å	11.349(4)	20.961(3)	20.960(2)	20.980(4)	20.929(2)
c, Å	16.962(6)	11.224(2)	11.212(1)	11.151(2)	11.140(1)
β, deg	108.938(5)	110.130(3)	110.295(2)	109.801(3)	110.264(2)
V, Å^3	2905.6(16)	2126.3(6)	2119.3(4)	2119.0(7)	2099.2(3)
Z	4	4	4	4	4
D_{calcd}, g cm^{-3}	1.473	1.567	1.580	1.587	1.621
abs coeff, mm^{-1}	3.590	3.699	3.918	4.145	4.642
scan angles in θ; min., max.	1.52, 24.99	1.94, 25.00	2.17, 25.00	1.94, 25.00	1.95, 25.00
T, K	213(2)	203(2)	213(2)	208(2)	203(2)
no. of data collected	18 578	15 783	11 024	14 071	15 543
unique reflctns	5043	3752	3727	3700	3693
no. of params refined	327	240	244	241	240
GOF	1.516	1.166	1.172	1.543	1.148
R_1 [$I > 2\sigma(I)$]	0.0430	0.0746	0.0247	0.0454	0.0770
wR_2 [$I > 2\sigma(I)$]	0.0897	0.1883	0.0602	0.0984	0.1848

[a] Graphite-monochromatized Mo Kα radiation, $\lambda = 0.71073$ Å; $R_1 = \sum||F_o| - |F_c||/\sum|F_o|$, $wR_2 = [\sum w(F_o{}^2 - F_c{}^2)^2/\sum w(F_o{}^2)^2]^{1/2}$, and $w = q/[\sigma^2(F_o{}^2) + (aP)^2 + bP]$. $P = [2F_c{}^2 + \max(F_c{}^2,0)]/3$.

Table 5. Crystallographic Data[a] for Complexes 22, 29, and 30 (all fw's are reported as monomer formula weights)

	22	**29**	**30**
formula	$C_{20}H_{48}B_8NdO_2Si_2$	$C_{22}H_{40}B_4ErOSi_2$	$C_{24}H_{46}B_4GdO_2Si_2$
fw	607.48	587.22	623.28
cryst syst	monoclinic	monoclinic	triclinic
space group	$C2/c$	$P2_1/n$	$P\bar{1}$
a, Å	23.323(5)	8.0829(9)	8.453(2)
b, Å	9.847(2)	23.889(3)	10.699(2)
c, Å	27.109(6)	14.814(2)	17.467(4)
α, deg	90	90	80.290(3)
β, deg	90.855(4)	102.081(2)	77.221(4)
γ, deg	90	90	87.107(4)
V, Å^3	6225(2)	2797.1(5)	1518.3(6)
Z	8	4	2
D_{calcd}, g cm^{-3}	1.296	1.394	1.363
abs coeff, mm^{-1}	1.760	3.097	2.281
scan angles in θ; min., max.	1.75, 25.00	1.64, 25.00	1.93, 25.00
T, K	173(2)	203(2)	213(2)
no. of data collected	11 820	20 870	10 585
unique reflctns	4646	4940	5143
no. of params refined	347	312	345
GOF	1.339	1.386	1.536
R_1 [$I > 2\sigma(I)$]	0.0894	0.0570	0.0589
wR_2 [$I > 2\sigma(I)$]	0.1882	0.0961	0.1171

[a] Graphite-monochromatized Mo Kα radiation, $\lambda = 0.71073$ Å; $R_1 = \Sigma||F_o| - |F_c||/\Sigma|F_o|$, $wR_2 = [\Sigma w(F_o^2 - F_c^2)^2 /\Sigma w(F_o^2)^2]^{1/2}$, and $w = q/[\sigma^2(F_o^2) + (aP)^2 + bP]$. $P = [2F_c^2 + \max(F_c^2,0)]/3$.

Table 6. Selected Bond Lengths (Å) for Complexes 3, 7−16, and 18−21

compd	Ln−X	Ln−C(1)	Ln−C(2)	Ln−B(3)	Ln−B(4)	Ln−B(5)	Ln−H(3)[a]	Ln−H(4)[b]	Ln−Cnt(1)[c]
3	2.5667(16)	2.714(6)	2.698(5)	2.703(7)	2.704(7)	2.720(6)	2.7265	2.7567	2.3635
7	2.644(3)	2.777(9)	2.773(9)	2.789(10)	2.788(10)	2.801(11)	2.7895	2.8153	2.4536
8	2.760(2)	2.730(19)	2.735(18)	2.73(2)	2.73(2)	2.74(2)	2.7041	2.7547	2.4103
9	2.5988(15)	2.739(5)	2.720(5)	2.744(6)	2.795(6)	2.746(6)	2.7381	2.7780	2.3955
10	2.5882(19)	2.731(7)	2.702(7)	2.727(7)	2.778(8)	2.728(8)	2.7545	2.7536	2.3766
11	2.5757(14)	2.707(5)	2.697(5)	2.708(6)	2.758(6)	2.714(6)	2.7317	2.7520	2.3573
12	2.531(3)	2.679(12)	2.650(11)	2.662(13)	2.711(15)	2.675(13)	2.7140	2.7405	2.3468
13	2.5544(12)	2.699(4)	2.673(4)	2.695(5)	2.734(5)	2.699(4)	2.7114	2.7253	2.3388
14	2.5427(15)	2.685(6)	2.662(5)	2.678(6)	2.723(7)	2.685(6)	2.6984	2.7176	2.3244
15	2.533(2)	2.688(8)	2.661(7)	2.671(9)	2.705(9)	2.679(9)	2.6962	2.7173	2.3166
16	2.5271(18)	2.686(6)	2.662(6)	2.663(7)	2.700(7)	2.668(7)	2.6742	2.7117	2.3119
18	2.599(2)	2.656(8)	2.654(8)	2.701(9)	2.775(9)	2.706(9)	2.6014	2.7981	2.3406
19	2.5835(10)	2.651(3)	2.660(4)	2.691(4)	2.745(4)	2.704(4)	2.6162	2.7966	2.3344
20	2.574(3)	2.642(8)	2.656(8)	2.674(9)	2.724(9)	2.680(9)	2.6364	2.7600	2.3209
21	2.556(3)	2.636(12)	2.642(13)	2.656(14)	2.759(15)	2.674(12)	2.5390	2.7778	2.3048

[a] For complexes of **18**, **19**, **20**, and **21**, the data are bond distances of Ln−H(5). [b] For complexes of **18**, **19**, **20**, and **21**, the data are bond distances of Ln−H(4). [c] Calculated data.

observed [$I > 2\sigma(I)$] were corrected for Lorentz, polarization, and absorption effects.[15] All structures were solved by direct methods and refined by full-matrix least-squares techniques using the SHELXTL system of programs.[16] All structures were refined on F^2 for all reflections.[16] Weighted wR_2 and goodness of fit (GOF) were based on F^2. The observed criterion of $I > 2\sigma(I)$ was used for the R-factor calculation. For **3** and **7**−**16**, nonsolvating THF molecules were present in each structure and located at the interval of the structure. In all of the structures, the non-H atoms were refined anisotropically. The nonsolvating and the solvated THF were disordered and were elastically restrained in the final stages of refinement. The carborane-cage H atoms of the compounds were located in ΔF maps whenever possible. The final values of R_1 and weighted wR_2 are listed in Tables 4 and 5. Selected interatomic distances and angles are listed in Tables 6−9, respectively. The detailed crystallographic parameters on all compounds can be seen in the Supporting Information, available on-line.

Results and Discussion

Syntheses. Reactions of the monosodium compound *nido*-1-Na(THF)-2,3-$(SiMe_3)_2$-2,3-$C_2B_4H_5$ (**1**) with anhydrous LnX_3 in a molar ratio of 2:1, in dry THF at 65 °C, produced dimerized half-sandwich lanthanacarborane complexes of formula [2,3-$(SiMe_3)_2$-1-X-1-$(THF)_m$-1-Ln(η^5-2,3-$C_2B_4H_4$)]$_2$•$(THF)_n$ (**3**, Ln = Y, X = Cl, $m = 2$, $n = 1$; **4**, Ln = La, X = Br; $m = 1$, $n = 0$; **5**, Ln = Ce, X = Br; $m = 1$, $n = 0$; **6**, Ln = Pr, X = Br; $m = 2$, $n = 0$; **7**, Ln = Nd; X = Cl, $m = 2$, $n = 1$; **8**, Ln = Sm; X = Br, $m = 2$, $n = 0$; **9**, Ln = Gd; X = Cl, $m = 2$, $n = 1$; **10**, Ln = Tb, X = Cl, $m = 2$, $n = 1$; **11**, Ln = Dy, X = Cl, $m = 2$, $n = 1$; **12**, Ln = Ho, X = Cl, $m = 2$, $n = 1$; **13**, Ln = Er, X = Cl, $m = 2$, $n = 1$; **14**, Ln = Tm, X = Cl, $m = 2$, $n = 1$; **15**, Ln = Yb, X = Cl, $m = 2$, $n = 1$; **16**, Ln = Lu X = Cl, $m = 2$, $n = 1$) as crystalline solids in 74−92% isolated yields, as shown in Table 1. The table also shows that essentially 1 equiv of the neutral carborane was also produced. The general synthetic procedure is outlined in Scheme 1. The method is based on a metathesis reaction between *nido*-1-Na(THF)-2,3-$(SiMe_3)_2$-2,3-$C_2B_4H_5$ (**1**) and LnX_3, with the driving force undoubtedly being the lower solubility of the NaX in THF compared to LnX_3. This is supported by the observation that the poorly soluble fluorides and chlorides of cerium and lanthanum failed to give product, while the more soluble

---

[15] Sheldrick, G. M. *SHELXTL, Version 5.1*; Bruker Analytical X-ray Systems*:* Madison, WI, 1997.

[16] Sheldrick, G. M. *SHELXL93*, program for the refinement of Crystal Structures; University of Göttingen: Germany, 1993.

Table 7. Selected Bond Lengths (Å) for Complexes of 22, 29, and 30

			22				
Nd−C(11)#1	2.747(13)	C(11)−B(15)	1.557(18)	C(22)−B(26)	1.69(2)	B(25)−B(26)	1.81(2)
Nd−C(12)#1	2.762(13)	C(11)−B(16)	1.73(2)	C(22)−B(23)	1.53(2)	Nd−H(14)	2.8318
Nd−B(13)#1	2.786(16)	B(13)−B(14)	1.63(2)	B(23)−B(24)	1.72(3)	Nd−H(15)	2.7859
Nd−B(14)#1	2.810(16)	B(13)−B(16)	1.76(2)	B(23)−B(26)	1.76(3)	Nd−H(24)	2.9695
Nd−B(15)#1	2.797(15)	B(14)−B(15)	1.64(2)	B(24)−B(25)	1.64(3)	Nd−H(25)	2.7877
Nd−B(24)	2.888(18)	B(14)−B(16)	1.80(2).	B(24)−B(25)	1.64(3)	Nd−Cnt(1A)	2.4380
Nd−B(25)	2.808(19)	C(21)−B(25)	1.54(2)	B(24)−B(26)	1.77(3)		
C(11)−C(12)	1.474(17)	C(21)−B(26)	1.73(2)	C(22)−B(26)	1.69(2)		
			29				
Er−C(31)	2.573(8)	C(1)−C(2)	1.468(9)	B(4)−B(6)	1.759(10)	C(33)−C(34)	1.36(2)
Er−C(32)	2.597(7)	C(1)−B(5)	1.697(9)	B(5)−B(6)	1.766(10)	C(34)−C(35)	1.31(2)
Er−C(33)	2.619(9)	C(1)−B(6)	1.697(9)	C(21)−C(25)	1.365(12)	Er−H(3)	2.6668
Er−C(34)	2.620(14)	C(2)−B(3)	1.515(9)	C(21)−C(22)	1.380(13)	Er−H(4)	2.8368
Er−C(35)	2.594(11)	C(2)−B(6)	1.741(9)	C(22)−C(23)	1.379(13)	Er−Cnt(2)	2.3473
Er−C(21)	2.621(8)	B(3)−B(4)	1.636(11)	C(23)−C(24)	1.378(13)	Er−Cnt(3)	2.3402
Er−C(22)	2.591(9)	B(4)−B(5)	1.750(11)	C(24)−C(25)	1.401(11)		
Er−C(23)	2.618(8)	B(3)−B(6)	1.795(11)	C(31)−C(35)	1.326(19)		
Er−C(24)	2.646(8)	B(4)−B(5)	1.750(11)	C(31)−C(32)	1.342(13)		
			30				
Gd−C(11)	2.599(11)	Gd−C(18)	2.582(12)	B(3)−B(4)	1.742(12)	C(23)−C(24)	1.378(13)
Gd−C(11)	2.599(11)	Gd−B(4)	2.779(9)	B(3)−B(6)	1.757(14)	C(23)−C(24)	1.378(13)
Gd−C(12)	2.592(10)	Gd−B(5)	2.851(8)	B(4)−B(5)	1.750(11)	C(24)−C(25)	1.401(11)
Gd−C(13)	2.593(9)	C(1)−C(2)	1.490(10)	B(4)−B(6)	1.759(10)	C(31)−C(35)	1.326(19)
Gd−C(14)	2.611(10)	C(1)−B(5)	1.534(11)	B(5)−B(6)	1.766(10)	C(31)−C(32)	1.342(13)
Gd−C(15)	2.602(11)	C(1)−B(6)	1.752(11)	C(21)−C(25)	1.365(12)	Gd−H(4)	2.7663
Gd−C(16)	2.603(11)	C(2)−B(3)	1.542(12)	C(21)−C(22)	1.380(13)	Gd−H(5)	2.9405
Gd−C(17)	2.581(12)	C(2)−B(6)	1.717(12)	C(22)−C(23)	1.379(13)	Gd−Cnt(1)	1.8575

Table 8. Bond Angles (deg) (calculated) for Complexes of 3, 7−16, and 18−21

compd	Cnt−Ln−X	Cnt−Ln−O(11)	Cnt−Ln−O(21)	Cnt−Ln−B(3)	Cnt−Ln−B(4)	Cnt−Ln−H(3)[a]	Cnt−Ln−H(4)[b]
3	106.069	174.690	102.400	99.220	99.850	103.240	104.576
7	106.291	173.313	101.069	98.096	99.052	101.940	104.056
8	106.620	173.072	101.437	98.286	99.92	102.131	105.659
9	106.087	174.245	101.868	98.917	99.872	102.872	104.844
10	106.094	174.524	102.341	98.912	99.816	102.826	104.738
11	105.978	174.750	102.470	98.901	99.823	102.705	104.713
12	105.878	174.860	102.655	99.399	100.325	103.318	105.332
13	105.859	174.996	102.734	99.434	100.133	103.455	104.909
14	105.949	175.084	103.096	99.449	100.199	103.341	104.994
15	105.772	175.295	103.125	99.593	100.204	103.439	104.744
16	105.739	175.489	103.189	99.886	100.362	103.895	104.870
18	105.123	103.736	176.268	99.431	100.654	106.053	103.990
19	105.036	103.822	176.733	99.923	100.461	104.918	103.578
20	104.829	103.871	177.088	99.812	100.700	105.834	104.511
21	105.244	103.953	176.283	99.860	101.233	106.754	104.466

[a] For complexes of **18**, **19**, **20**, and **21**, the data are bond angles of Cnt−Ln−H(4). [b] For complexes of **18**, **19**, **20**, and **21**, the data are bond angles of Cnt−Ln−H(5).

bromides gave **4** and **5** in yields of 92% and 88%, respectively. In the reactions, the second carborane monoanion acts as a mild base (proton sponge) and assists the removal of the bridged hydrogen on the complexing carborane. The presence of a strong base, such as BuLi, leads to complications such as THF degradation, as observed earlier.[5] However, since the neutral carborane coproduct can be recycled, the method shown in Scheme 1 does not suffer from any undue inefficiency (reference to Table 1 shows that there is over 90% recovery of the carborane, either in the complex or as the neutral carborane). An inspection of Table 1 shows that the method is applicable to all of the naturally occurring 4f metals with the exception of europium. The desired product could not be obtained when europium halide was reacted with **1** due to the reduction of Eu(III) to Eu(II) by **1**. However, that does not seem to be a problem with La, Ce, Sm, and Yb, which also have stable +2 valences. Substitution of one of the TMS groups by a Me on the ligand did not significantly affect the reactivity of the ligand toward lanthanide halides; high yields (72−80%) of corresponding products of [2-Me-3-(SiMe$_3$)-1-Cl-1-(THF)$_2$-Ln(η^5-2,3-$C_2B_4H_4$)]$_2$ (**17**, Ln = Nd; **18**, Ln = Dy; 1**9**, Ln = Ho; **20**, Ln = Er; **21**, Ln = Yb) were obtained as crystalline solids (see Scheme 1). A comparison of the yields for a given lanthanide shows that, generally, those from the bis(trimethylsilyl)carborane (**1**) are higher than those from the Me/SiMe$_3$-pendent carborane (**2**) (see Table 1). As one progresses from Nd to Yb, the difference becomes less and less, until with Yb the yields are reversed. This may be a result of the decrease in the ionic radius of the metal ions with increasing atomic number, which makes steric factors more and more important. It should be noted that these are very clean reactions, giving the half-sandwich products in high yields across the 4f period; this is not usually the case. There are numerous examples in both the large and small-cage carboranes of the syntheses of quite different structures for metallacarboranes formed from similar metals under almost identical reaction conditions. For example a 1:1 molar ratio reaction of $LaCl_3$ and $Na_2C_2B_9H_{11}$ gave only the full-sandwich [Na(THF)$_2$][($C_2B_9H_{11}$)$_2$La(THF)$_2$], while the smaller lanthanides (Ln = Y, Er, Yb, Lu) produced the expected half-sandwich compounds ($C_2B_9H_{11}$)Ln(THF)$_2$(μ-Cl)$_2$Na(THF)$_2$.[4a] Indeed, the initial interest in the small-cage lanthanacarboranes stemmed from the unexpected half-sandwich trinuclear clusters that were

Table 9. Selected Bond Angles (deg) for Compounds 22, 29, and 30

		22			
O(31)−Nd−O(41)	74.5(3)	B(15)−Nd−B(14)	34.0(4)	Cnt(A)−Nd−H(15)	102.106
O(31)−Nd−B(15)	94.1(4)	B(25)−Nd−B(14)	100.4(5)	Cnt(A)−Nd−H(14)	101.397
O(41)−Nd−B(15)	78.3(4)	O(31)−Nd−B(24)	89.5(4)	Cnt(A)−Nd−B(24)	107.885
O(31)−Nd−B(25)	122.1(4)	O(41)−Nd−B(24)	77.7(4)	Cnt(A)−Nd−B(25)	107.140
O(41)−Nd−B(25)	81.5(4)	Cnt(A)−Nd−O(41)	170.899	Cnt(A)−Nd−H(24)	103.190
B(15)−Nd−B(25)	131.4(5)	Cnt(A)−Nd−O(31)	97.964	Cnt(A)−Nd−H(25)	100.794
O(31)−Nd−B(14)	127.4(4)	Cnt(A)−Nd−B(15)	97.463		
O(41)−Nd−B(14)	83.7(4)	Cnt(A)−Nd−B(14)	97.333		
		29			
O(11)−Er−B(3)	114.2(2)	C(21)−Er−B(3)	75.7(3)	Cnt(2)−Er−H(4)	127.180
C(31)−Er−B(3)	107.2(4)	O(11)−Er−C(22)	126.7(3)	Cnt(3)−Er−O(11)	106.840
C(22)−Er−B(3)	92.3(3)	O(11)−Er−C(35)	127.3(5)	Cnt(3)−Er−B(3)	105.872
C(35)−Er−B(3)	82.6(4)	O(11)−Er−C(23)	103.9(3)	Cnt(3)−Er−B(4)	105.684
C(32)−Er−B(3)	131.5(3)	Cnt(2)−Er−O(11)	100.277	Cnt(3)−Er−H(3)	106.966
C(23)−Er−B(3)	122.5(3)	Cnt(2)−Er−B(3)	102.374	Cnt(3)−Er−H(4)	105.218
C(33)−Er−B(3)	116.6(4)	Cnt(2)−Er−B(4)	122.486	Cnt(2)−Er− Cnt(3)	127.597
C(34)−Er−B(3)	87.3(5)	Cnt(2)−Er−H(3)	83.466		
		30			
O(31)−Gd−O(21)	77.97(17)	C(12)−Gd−C(11)	29.9(4)	B(4)−Gd−B(5)	33.5(3)
C(17)−Gd−C(18)	31.9(6)	C(13)−Gd−C(11)	57.7(4)	Cnt−Gd−O(21)	123.783
C(17)−Gd−C(12)	80.3(5)	O(31)−Gd−B(4)	90.3(2)	Cnt−Gd−O(31)	129.776
C(18)−Gd−C(12)	58.2(5)	O(21)−Gd−B(4)	76.3(3)	Cnt−Gd−B(4)	135.925
C(17)−Gd−C(13)	88.6(4)	C(17)−Gd−B(5)	116.6(6)	Cnt−Gd−B(5)	132.376
C(18)−Gd−C(13)	79.4(4)	C(18)−Gd−B(5)	95.1(4)	Cnt−Gd−H(4)	123.953
C(12)−Gd−C(13)	30.5(4)	C(12)−Gd−B(5)	98.4(3)	Cnt−Gd−H(5)	118.947
O(31)−Gd−C(11)	128.0(4)	C(13)−Gd−B(5)	120.7(3)		

Scheme 1. Syntheses of Half-Sandwich Halolanthanacarboranes

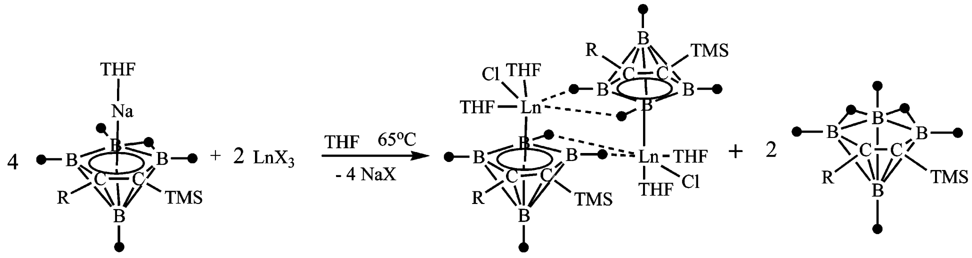

●=H
X = Cl, Br
R = -SiMe$_3$ for complexes of **3**, **8-16**
R = Me for complexes of **18-21**

formed under stoichiometric conditions that were conducive to full-sandwich complex formation.[5] For this reason the systematic studies on the syntheses of the small-cage lanthanacarboranes have involved the full-sandwich complexes.[6,7,9] Although there have been isolated reports of half-sandwich lanthanacarboranes in the C_2B_4 cage system,[8,17] including an interesting mixed half-sandwich neodymacarborane cation/full-sandwich neodymacarborane anion salt,[18] the present report is the only one describing a systematic, generally applicable, high-yield synthetic route to the half-sandwich lanthanacarboranes. The net approach outlined in Scheme 1 is not fundamentally different from other methods starting with the monoanions [*nido*-$R_2C_2B_4H_5$]$^-$ and [*nido*-$R_2C_2B_9H_{10}$]$^-$, that is, first remove the second bridged hydrogen and then add a capping metal group.[3,19] Retention of the bridge hydrogen most often leads to *exo*-polyhedral complexes (vide infra).[3,19,20] The novelty of the present method is in using a second *nido*-1-Na(THF)-2,3-$(SiMe_3)_2$-2,3-$C_2B_4H_5$ (**1**) as the proton scavenger. Its use prevents complications inherent in the use of strong bases, and it controls the amount of proximate carborane available in the reaction mixture, thus discouraging ligand redistribution reactions.[3,4]

The lanthanide source in Scheme 1 was LnX_3, and all the half-sandwich Ln(III) products have halide ions. The reactivity of the metal-bound halides is demonstrated in Scheme 2, which shows that the reactions of [2-Me-3-$(SiMe_3)$-1-Cl-1-$(THF)_2$-1-Ln(η^5-2,3-$C_2B_4H_4$)]$_2$ (**17**, Ln = Nd; **19**, Ln = Ho; **20**, Ln = Er) with 1 equiv of **2** produced the unusual half-sandwich lanthanacarboranes {2-Me-3-$(SiMe_3)$-1-[4,5-(μ-H)-*nido*-2-Me-3-$(SiMe_3)$-2,3-$C_2B_4H_4$]-1-Ln(η^5-2,3-$C_2B_4H_4$)}$_m$·n(THF) (**22**, Ln = Nd, m = 2, n = 2; **23**, Ln = Ho, m = 3, n = 8; **24**, Ln = Er, m = 2, n = 1) as crystalline solids in 70−81% yield, as noted in Scheme 2 and verified by the crystal structure of **22** (see Figure 3). The compounds arise from the formal substitution of a Cl$^-$ by [*nido*-2-Me-3-$(SiMe_3)$-2,3-$C_2B_4H_5$]$^-$; there was no trace of a full-sandwich compound. Complexes **22**−**24** could also be obtained directly by the reaction of **2** with corresponding $LnCl_3$ at 60 °C in molar ratios of 3:1 in dry THF in 76−80%

---

(17) Hosmane, N. S.; Oki, A. R.; Zhang, H. *Inorg. Chem. Commun.* **1998**, *1*, 101−104.

(18) Wang, J.; Li, S.; Zheng, C.; Maguire, J. A.; Hosmane, N. S. *Inorg. Chem. Commun.* **2003**, *6*, 549−552.

(19) For general references see: (a) Grimes, R. N. In *Comprehensive Organometallic Chemistry II*; Abel, E. W., Stone, F. G. A., Wilkinson, G., Eds.; Elsevier Science: New York, 1995; Vol. 1. (b) Saxena, A. K.; Maguire, J. A.; Hosmane, N. S. *Chem. Rev.* **1997**, *97*, 2421−2461, and references therein.

(20) Hosmane, N. S.; Zhu, D.; McDonald, J. E.; Zhang, H.; Maguire, J. A.; Gray, T. G.; Helfert, S. C. *Organometallics* **1998**, *17*, 1426−1437.

Scheme 2. Reactivity of Half-Sandwich Halolanthanacarboranes

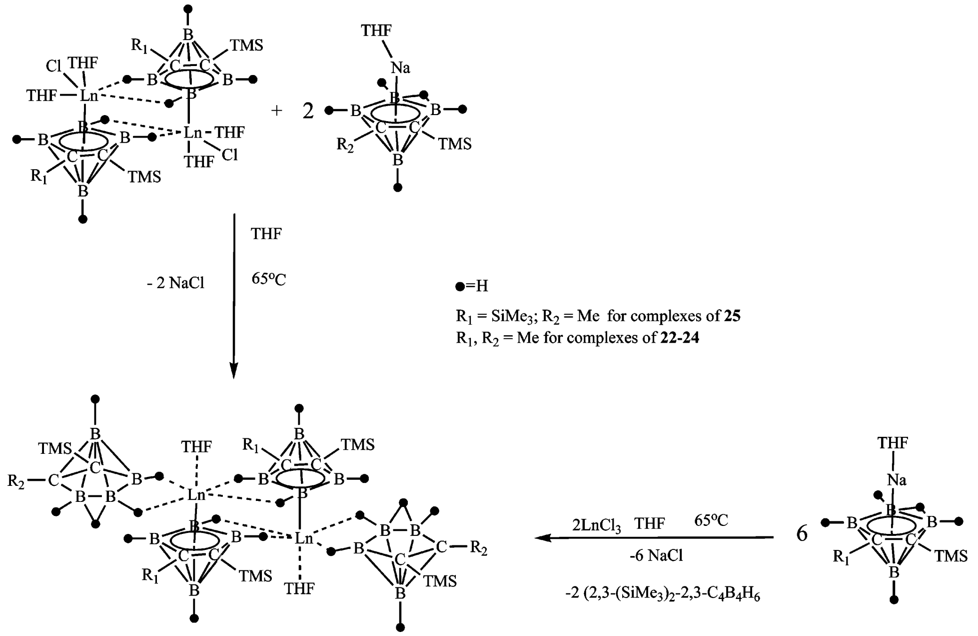

Scheme 3. Syntheses of Mixed-Ligand Lanthanacarborane Complexes

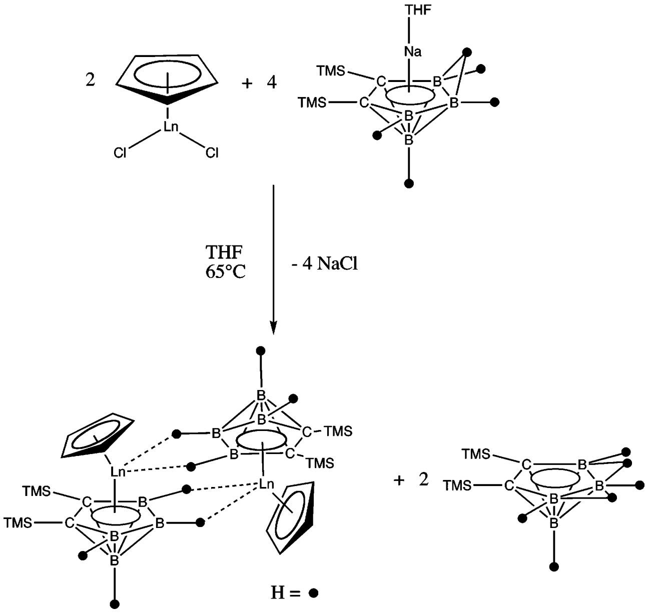

Scheme 4. Synthesis of Erbacarborane {(η^5-C$_5$H$_5$)$_2$-1-Er[4,5-(μ_2-H)-2,3-(SiMe$_3$)$_2$-2,3-C$_2$B$_4$H$_4$]}·(THF) (29)

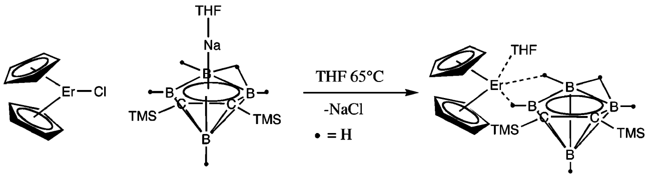

Scheme 5. Synthesis of Gadolinacarborane {(η^8-C$_8$H$_8$)-1-Gd[4,5-(μ-H)-2,3-(SiMe$_3$)$_2$-2,3-C$_2$B$_4$H$_4$]}·2(THF) (30)

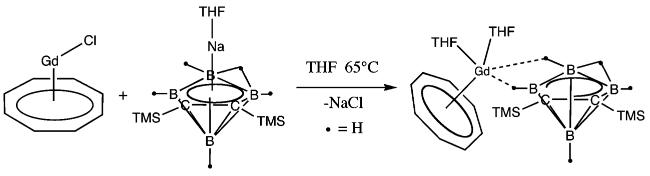

yield (see Scheme 2). These results emphasize the delicate balance of forces that determine the products; the 3:1 carborane-to-LnCl$_3$ stoichiometry could just as well have led to an equimolar mixture of a half-sandwich lanthanacarborane cation and a full-sandwich lanthacarborane anion, along with three neutral carboranes. The half-sandwich-cation/full-sandwich-anion carbons-apart neodymacarborane, {[*closo*-1-Nd-(μ-H)$_6$-2,4-(SiMe$_3$)$_2$-2,4-C$_2$B$_4$H$_4$]$^+$[1,1′-(THF)$_2$-2,2′,4,4′-(SiMe$_3$)$_4$-5,5′,6,6′-(μ-H)$_4$-1,1′-*commo*-(η^5-2,4-C$_2$B$_4$H$_4$)$_2$]$^-$}$_2$ has been reported.[18] The mixed coordinate complex {2,3-(SiMe$_3$)$_2$-1-[4,5-(μ-H)-(*nido*-2-Me-3-(SiMe$_3$)-2,3-C$_2$B$_4$H$_4$)]-1-Gd(η^5-2,3-C$_2$B$_4$H$_4$)}$_2$·3(THF) (**25**) was obtained in good yield from the reaction of **9** with **2** (see Scheme 2). It is of interest to note that the Ho compound, **23**, is the only trimeric lanthanacarborane isolated in this study. Since its trimeric nature was determined by chemical analysis rather than crystal structure determination, it is not possible to determine what structural features support the trimer formation.

The effect of the number of chlorides originally on the metal center was studied by reacting (η^5-Cp)LnCl$_2$, (η^5-Cp)$_2$LnCl, and (η^8-C$_8$H$_8$)LnCl with **1**. The mixed-ligand sandwich complexes [1-(η^5-C$_5$H$_5$)-2,3-(SiMe$_3$)$_2$-1-Ln(η^5-2,3-C$_2$B$_4$H$_4$)]$_2$·*n*(THF) (**26**, Ln = Tb, $n = 2$; **27**, Ln = Dy, $n = 2$; **28**, Ln = Er, $n = 3$) were obtained as crystalline solids in 70−92% isolated yields by the reactions of **1** with CpLnCl$_2$ in a molar ratio of 2:1, as shown in Scheme 3. These can be thought of as being related to **10**, **11**, and **13** by the formal replacement of a chloride by a cyclopentadienide. On the other hand, the monochlorolanthanides (Cp)$_2$ErCl and (η^8-C$_8$H$_8$)GdCl reacted with **1** to give the *exo*-coordinated lanthanacarborane complexes *exo*-4,5-(Cp)$_2$Er[2,3-(SiMe$_3$)$_2$-2,3-C$_2$B$_4$H$_5$]·(THF) (**29**) and *exo*-4,5-(η^8-C$_8$H$_8$)Gd[2,3-(SiMe$_3$)$_2$-2,3-C$_2$B$_4$H$_5$]}·2(THF) (**30**), respectively, in good yields (see Schemes 4 and 5). In both **29** and **30** the presence of the bridged hydrogen on the carborane led to the metal occupying bridging positions rather than apical ones. This has generally been found to be the case for main group,[20] transition metal,[21] and lanthanide[3b] carborane complexes. The

Scheme 6. Proposed Mechanism for the Formation of Half-Sandwich Halolanthanacarboranes

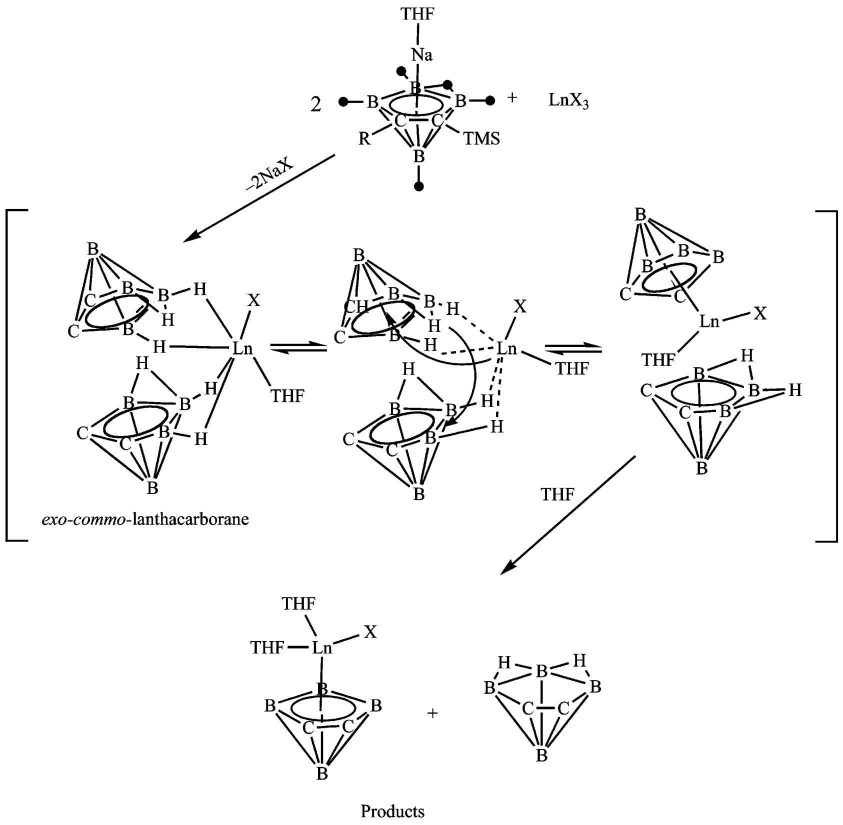

exceptions are the group 1 half-sandwich carborane complexes, such as **1** and **2**, and the full-sandwich lithiacarborane [Li$^+$-(TMEDA)$_2$][*commo*-1,1′-Li{2,3-(SiMe$_3$)$_2$-2,3-C$_2$B$_4$H$_5$}$_2$], where X-ray structures show the metals occupy apical positions above the C$_2$B$_3$ faces.[11,22,23] It should be noted that, on standing, the half-sandwich group 1 carboranes reverted to their respective *exo*-metallacarboranes.[24,25]

The mechanism for the reactions shown in Scheme 1 is not known. What is known is that the reactions seem to require at least two halides on the lanthanide precursor and a 2:1 carborane-to-Ln molar ratio. A reasonable sequence of steps would involve the initial precipitation of 2 equiv of NaCl by a 1:2 molar ratio reaction of LnCl$_3$ and **1**, leading to the formation of an *exo-commo*-lanthanacarborane intermediate, as shown in Scheme 6. The intermediate could then undergo an intramolecular proton transfer, producing the half-sandwich halolanthanacarborane and the neutral *nido*-carborane product. The compound *commo-exo*-4,4′,5,5′-Mg(TMEDA)[2-Me-3-(SiMe$_3$)-2,4-C$_2$B$_4$H$_5$]$_2$ has been isolated and found to have a structure similar to the one proposed in Scheme 6.[20] While there is no direct verification of this mechanism, it does at least explain the stoichiometry requirements, and the proposed intermediate does have precedence in the literature.

Crystal Structures. Because of the generality of the reaction processes and in order to obtain structural information on a series of related compounds, the X-ray diffraction analyses were performed on a number of half-sandwich halolanthanacarboranes. As expected, the bis(trimethylsilyl)-pendent half-sandwich lanthanacarboranes (**3**, **7**−**16**) are isostructural, as are the Me/SiMe$_3$-substituted lanthanacarborane analogues, **18**−**21**. A general structure for compounds **3** and **7**−**16** is given in Figure 1, and that of **18**−**21** is shown in Figure 2. Table 6 is a list of some important bond distances, and Table 8 gives some selected bond angles. A more complete listing can be found in the Supporting Information. All structures are dimeric in which each Ln(III) is η^5-bonded by a carborane dianion, two THF molecules, and a halide In addition, a neighboring carborane moiety

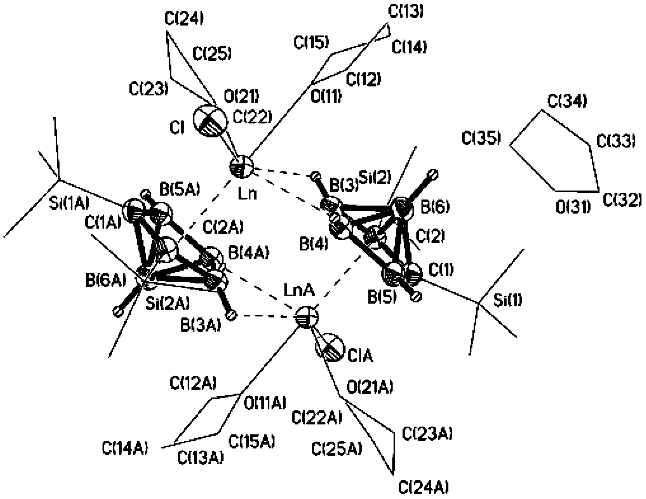

Figure 1. Perspective view of half-sandwich lanthanacarboranes of formula [2,3-(SiMe$_3$)$_2$-1-X-1-(THF)$_m$-1-Ln(η^5-2,3-C$_2$B$_4$H$_4$)]$_2$·*n*(THF) (**3**, **7**−**16**). Thermal ellipsoids are drawn at the 50% probability level. The solvated THF molecules and the *exo*-polyhedral SiMe$_3$ groups are drawn with thin lines.

---

(21) (a) Hosmane, N. S.; Grimes, R. N. *Inorg. Chem.* **1979**, *18*, 2886. (b) Yang, J.; Zheng, C.; Maguire, J. A.; Hosmane, N. S. *Inorg. Chem. Commun.* **2004**, *7* (1), 111−113.

(22) Hosmane, N. S.; Siriwardane, U.; Zhang, G.; Zhu, H.; Maguire, J. A. *Chem. Commun.* **1989**, 1128−1130.

(23) Hosmane, N. S.; Tang, J.; Zhang, H.; Maguire, J. A. *J. Am. Chem. Soc.* **1996**, *118*, 5150−5151.

(24) Wang, Y.; Zhang, H.; Maguire, J. A.; Hosmane, N. S. *Organometallics* **1993**, *12*, 3781−3784.

(25) Hosmane, N. S.; Jia, L.; Wang, Y.; Saxena, A. K.; Zhang, H.; Maguire, J. A. *Organometallics* **1994**, *13*, 4113−4116.

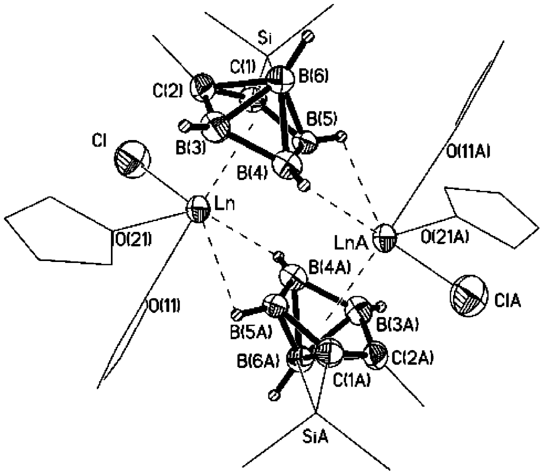

Figure 2. Perspective view of half-sandwich lanthanacarboranes of formula [2-Me-3-(SiMe$_3$)-1-X-1-(THF)$_m$-1-Ln(η^5-2,3-C$_2$B$_4$H$_4$)]$_2$·*n*(THF) (**18**−**21**). Thermal ellipsoids are drawn at the 30% probability level. The solvated THF molecules and the *exo*-polyhedral SiMe$_3$ groups are drawn with thin lines.

is bonded to the metal through a set of two Ln−H−B bonds (see Figures 1 and 2). An inspection of Figures 1 and 2 and reference to Table 8 show that the local geometry about each Ln is best described as a distorted trigonal bipyramid in which the η^5-bonding carborane and one of the THF molecules occupy the axial positions, with the Cnt−Ln−O angles ranging from 173° (**8**) to 177° (**20**), and the other THF molecule, the halide ion, and the η^2-bonding carborane residing in the trigonal plane. The other ligands are directed away from the η^5-bonded carborane, with the average O(21)−Ln−O(11) angle being 74° and the Cnt−Ln−Cl angles averaging 106°. The average Ln−Cnt distances decrease in the order **7** (Nd) (2.4536 Å) > **8** (Sm) (2.4103 Å) > **9** (Gd) (2.3955 Å) > **10** (Ho) (2.3766 Å) > **11** (Dy) (2.3573 Å) > **12** (Ho) (2.3468 Å) > **13** (Er) (2.3388 Å) > **14** (Tm) (2.3244 Å) > **15** (Yb) (2.3166 Å) > **16** (Lu) (2.3119 Å). For the same metal these distances are essentially the same as those found in the trinuclear lanthanacarborane clusters[5c] and the corresponding full-sandwich lanthanacarboranes.[6] A decrease in this Ln−ligand distance with an increase in the Ln atomic number parallels the decrease in the metal's "ionic radii" and is consistent with essentially electrostatic metal−carborane interactions. This same trend has been noted in the lanthanocenes.[26]

The X-ray crystal structure of **22**, formed from an equimolar reaction of [2-Me-3-(SiMe$_3$)-1-Cl-1-Nd(η^5-2,3-C$_2$B$_4$H$_4$)]$_2$·4(THF) (**17**) with *nido*-1-Na(THF)-2-Me-3-(SiMe$_3$)-2,3-C$_2$B$_4$H$_5$ (**2**), is shown in Figure 3. The compound crystallizes as a dimer with a structure similar to **7** except for the replacement of one SiMe$_3$ on each carborane with an Me group and the substitution of the Cl$^-$ by a [2-Me-3-(SiMe$_3$)-2,3-C$_2$B$_4$H$_5$]$^-$. Each Nd is bonded to two THF molecules, an η^5-coordinating carborane, and two η^2-bonding carboranes. The Cnt−Nd distance in **22** (2.4380 Å) is essentially the same as found in **7** (2.4536 Å). At least as measured by the Nd−B(24,25) and the Nd−(B14,15) distances, the two η^2-bonding carboranes seem to interact equally with the Nd, irrespective of whether they are bonded to another Nd or a bridged hydrogen (see Figure 3 and Table 7).

The X-ray crystal structures of complexes **29** and **30** are shown in Figures 4 and 5, respectively. Both structures are monomeric, with the (Cp)$_2$Er(THF) or (C$_8$H$_8$)Gd(THF) groups bonding *exo*-polyhedrally through two Ln−H−B bonds. Although they could not be located in the electron density maps, each carborane also contains a bridged hydrogen. A comparison of the facial B−B bond distances in the compounds shows that the distances between the pair of boron atoms that coordinate to the Ln groups are over 0.1 Å shorter than the other B−B distances; this has been observed in other *exo*-polyhedrally bonded metallacarboranes, where it was found that the larger B−B bond distance is associated with a bridged hydrogen.[11,20,25]

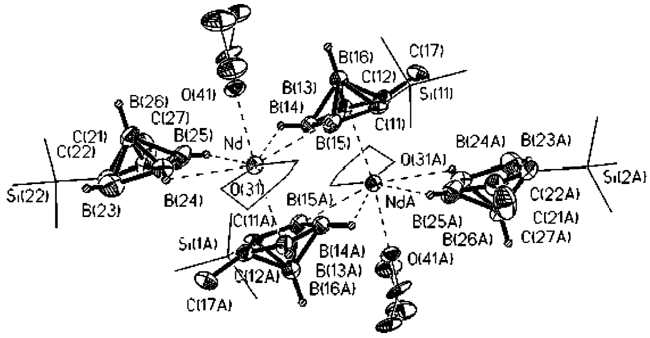

Figure 3. Perspective view of lanthanacarborane **22**. Thermal ellipsoids are drawn at the 50% probability level. The solvated THF and TMEDA molecules and the *exo*-polyhedral SiMe$_3$ groups are drawn with thin lines.

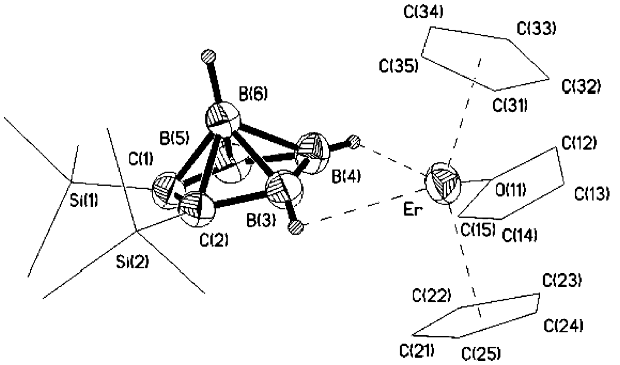

Figure 4. Perspective view of erbacarborane **29**. Thermal ellipsoids are drawn at the 50% probability level. The solvated THF molecules and the *exo*-polyhedral SiMe$_3$ groups are drawn with thin lines.

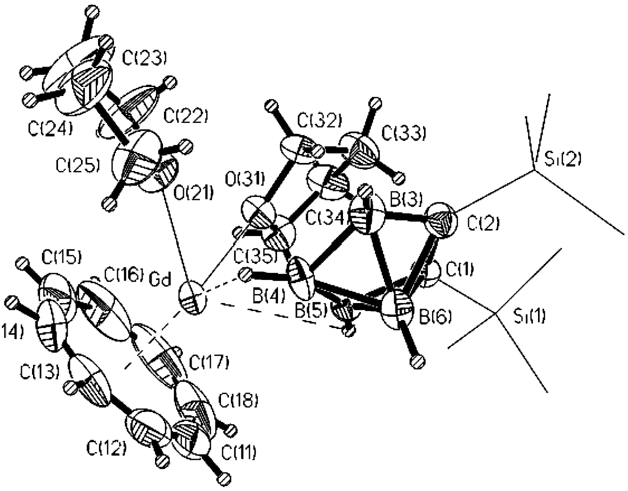

Figure 5. Perspective view of gadolinacarborane **30**. Thermal ellipsoids are drawn at the 50% probability level. The solvated THF molecules and the *exo*-polyhedral SiMe$_3$ groups are drawn with thin lines.

---

(26) (a) Maginn, R. E.; Manastyrkyj, S.; Dubeck, M. *J. Am. Chem. Soc.* **1963**, *85*, 672−675. (b) Raymond, K. N.; Eigenbret, C. W., Jr. *Acc. Chem. Res.* **1980**, *13*, 276.

Spectroscopy. All compounds were characterized by IR spectroscopy and elemental analyses. Except that the analytical samples contain different numbers of THF molecules in some of the complexes, the results of these analyses are consistent with the crystal structures. The IR spectra of the lanthanacarboranes all exhibit well-resolved multiple terminal B−H stretching vibrations in the 2270−2590 cm^{-1} range. Such fine structures of B−H stretching bands have been previously observed in other lanthanacarboranes and have been explained on the basis of unequal interactions of the boron-bound hydrogens with the *exo*-polyhedrally bound metal groups present in the complex.[5−7]

Because of the strong paramagnetism of complexes **5**−**15**, **18**−**21** **22**, **29**, and **30**, no useful NMR spectra could be obtained. However, the diamagnetic yttrium (**3**), lanthanum (**4**), and lutetium (**16**) complexes gave interpretable NMR data. The ^{1}H, ^{13}C, and ^{11}B NMR spectra are all consistent with the formulas given in Scheme 1 and, for **3** and **16**, their crystal structures. Neither the terminal B−H hydrogens nor the cage carbons were detectable in the NMR. The only thing of note is that both the ^{1}H and the ^{13}C NMR spectra of **3** show unequivalent $SiMe_3$ groups, while the spectra of **4** and **16** show equivalent $SiMe_3$ groups. Since compounds **3** and **16** were found to be isostructural by X-ray analysis, there is no ready explanation for these spectral differences. The ^{11}B NMR spectra showed three resonances with 1:2:1 peak area ratios at δ 11.9, −0.77, and −52.7 ppm for **3**, at δ 13.34, −1.15, and −51.8 ppm for **4**, and at δ 25.9, −1.01, and −52.7 ppm for **16**. The most downfield shifted resonances, in the δ 25.9 to 11.9 ppm region, are assigned to the unique boron (B(4) in Figure 1), the resonances at δ −0.77 to −1.15 ppm to the other two basal borons, and those in the δ −51.8 to −52.7 ppm region to the apical borons. Because of the terminal hydrogens, all should be doublets; however only those of the apical borons are sharp enough so that the splitting can be observed.

Conclusions

A highly efficient synthesis of half-sandwich halolanthanacarboranes of the formulas $[2\text{-R-3-(SiMe}_3)\text{-1-X-1-(THF)}_m\text{-1-Ln-}(\eta^5\text{-2,3-C}_2B_4H_4)]_2\cdot n(\text{THF})$ has been developed using the reactions of *nido*-1-Na(C_4H_8O)-2,3-($SiMe_3$)$_2$-2,3-$C_2B_4H_5$ (**1**) or *nido*-1-Na(C_4H_8O)-2-Me-3-($SiMe_3$)-2,3-$C_2B_4H_5$ (**2**) with LnX_3 in 2:1 molar ratios. The halides of the half-sandwich lanthanacarboranes were found to be chemically active in that they could be replaced by [*nido*-2-Me-3-($SiMe_3$)-2,3-$C_2B_4H_5$]$^{-}$ to give {2-Me-3-($SiMe_3$)-1-[4,5-(μ-H)-*nido*-2-Me-3-($SiMe_3$)-2,3-$C_2B_4H_4$]-1-Ln(η^5-2,3-$C_2B_4H_4$)}$_m\cdot n$(THF). It was found that $CpLnCl_2$ (Ln = Tb, Dy, and Er) react with **1** to give [(η^5-C_5H_5)Ln(2,3-($SiMe_3$)$_2$-2,3-$C_2B_4H_4$)]$_2\cdot n$(THF). On the other hand, the reaction of $(Cp)_2ErCl$ and $(C_8H_8)GdCl$ with **1** produced the *exo*-lanthanacarboranes *exo*-(η^5-C_5H_5)$_2$Er[4,5-(μ-H)-2,3-($SiMe_3$)$_2$-2,3-$C_2B_4H_4$]}·(THF) and *exo*-(η^8-C_8H_8)Gd[4,5-(μ-H)-2,3-($SiMe_3$)$_2$-2,3-$C_2B_4H_4$]}·2(THF), respectively. An intramolecular H transfer reaction mechanism of an initially formed *exo-commo*-lanthanacarborane was proposed to explain the products. It is important to note that due to recent synthetic advances, small-cage metallacarborane chemistry is now generally accessible.[27]

Acknowledgment. This work was supported by grants from the National Science Foundation (CHE-0241319), the donors of the Petroleum Research Fund, administered by the American Chemical Society, The Robert A. Welch Foundation (N-1322 to J.A.M.), and Northern Illinois University through a Distinguished Research Professorship. N.S.H. gratefully acknowledges the Forschungspreis der Alexander von Humboldt-Stiftung and the Gauss Professorship of the Göttingen Academy of Sciences.

Supporting Information Available: Tables of crystallographic data, including fractional coordinates, bond lengths and angles, anisotropic displacement parameters, and hydrogen atom coordinates, of **3**, **7**−**16**, **18**−**21**, **22**, **29**, and **30**. This material is available free of charge via the Internet at http://pubs.acs.org.

OM060268K